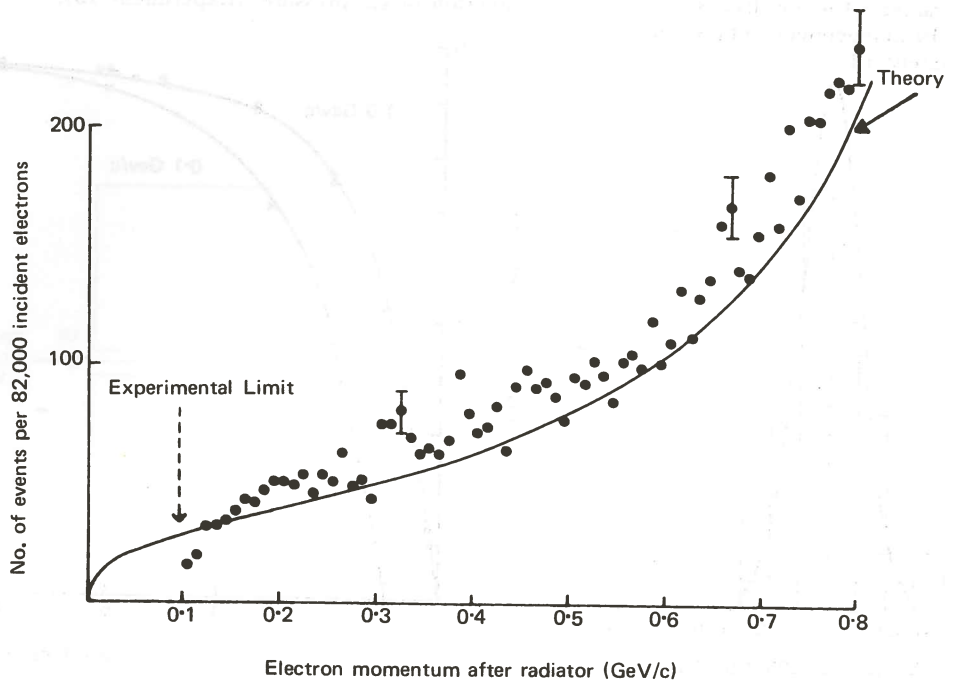

Figure 39. Electron momentum spectrum after passing through 0·91 radiation lengths of carbon. The solid line is a theoretical curve, normalised to incident electron flux and not to the experimental points.

The second part of the investigation consisted of measurements of the momenta of individual electrons both before and after they had passed through one of a variety of radiators (carbon, copper, etc). The ratio of the two can be compared with the predictions of the bremsstrahlung theory. The measurements were made using sonic spark chambers in two magnetic spectrometers working on-line to a DDP 516 computer. A preliminary analysis of each event was made within 20 milliseconds of its occurrence and up-to-date histograms produced for display. Records for approximately 200,000 events were also written on magnetic tape for subsequent detailed analysis. The number of electrons incident on the radiators during the course of the experiment was about 500,000. No effect comparable to that reported in the bubble chamber experiment has been found; see figure 39.

Final results are not yet available but it already appears that no breakdown of quantum electrodynamics, or evidence for a new light particle will be found in this experiment.

Experiment 16

WESTFIELD COLLEGE, LONDON
UNIVERSITY OF SUSSEX
RUTHERFORD LABORATORY

Search for Charge Asymmetry in Eta Decay

An important insight into the interaction processes that occur in elementary particle physics can be gained by applying and studying certain symmetry principles. One asks whether the laws of physics remain unchanged when, for example, a set of interacting particles are replaced by the equivalent set of anti-particles (the operation C), or time is made to run backwards (the operation T), or the world is viewed as reflected in a mirror (the parity operation P). The surprising result of experiments testing these symmetry rules is that for the weak interaction the operations C, P, or CP each produce a new physical situation with different physical behaviour. As a result of these findings our understanding of the weak interaction has changed considerably.

There are now indications that the electromagnetic interaction may also lack symmetry under the particle – antiparticle interchange operation C. If this result were confirmed, it would have a fundamental impact on our model of the electromagnetic interaction, which is thought to be very well understood and symmetric under C.

This experiment tests C symmetry in the electromagnetic interaction by looking at the decay of the eta meson:

$$\eta \rightarrow \pi^+ \pi^- \pi^\circ$$

The π^+ and π^- are particle and antiparticle, and C symmetry requires that nature should treat them both with equal respect. Thus if:

$N^+ = N(E^+ > E^-)$ i.e. the number of times the π^+ is more energetic than the π^-, and

$N^- = N(E^- > E^+)$, then C symmetry implies:

$$A = \frac{N^+ - N^-}{N^+ + N^-} = 0$$

The most recently published value for this quantity is:

$$A = 1{\cdot}5\% \pm 0{\cdot}5\%$$

for a measured sample of 36,000 η decay events. This is a result with three standard deviations of significance, and clearly requires confirmation.

The $\pi 8$ group have set out to repeat this experiment and hope to obtain approximately ten times as many events. The apparatus being used is shown in figure 40. The η mesons to be studied are produced in the process $\pi^- p \rightarrow \eta n$ and are selected from unwanted background by measuring the time of flight of the neutron from the target to the ring of 60 neutron counters. An array of spark chambers surrounds the hydrogen target and the whole is situated in a large electromagnet. This allows the π^+ and π^- mesons from the η decay to be detected and have their energies measured.

Data taking started in September and to date a total of 600,000 events have been recorded on magnetic tape. This represents about 20% of the final expected total. A preliminary analysis using simple helix fitting in a uniform magnetic field to determine the decay pion momenta indicates that some 12% of the events recorded are useful η decays.

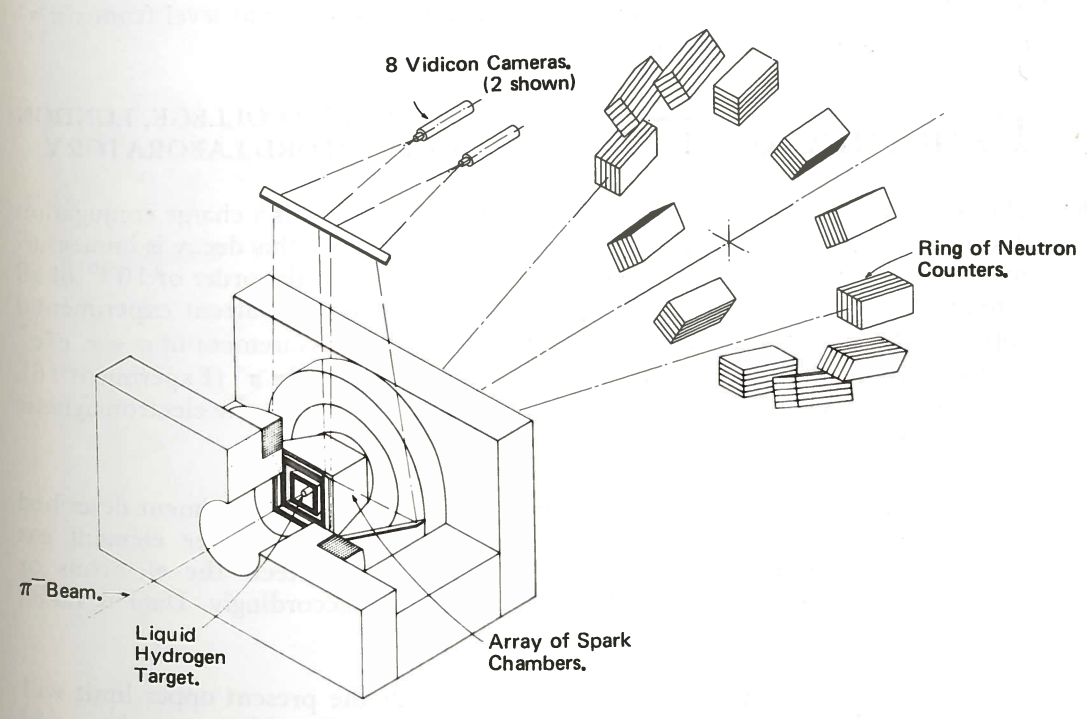

Figure 40. Schematic diagram of the apparatus used in Experiment 16 to study η decay.

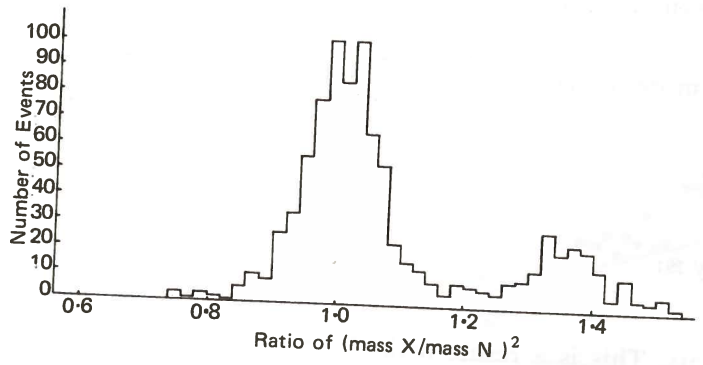

Figure 41. Plot of [(mass X)/(mass neutron)]^2 where X is the total missing neutral mass in the reaction $\pi^-p \rightarrow \pi^+\pi^-X$. (Experiment 16).

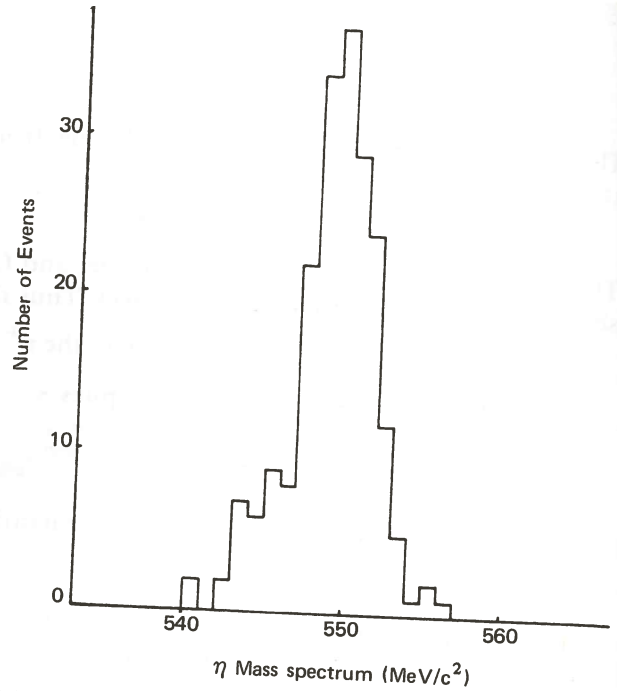

Figure 42. Mass distribution of Z for the reaction $\pi^-p \rightarrow nZ$ for events identified as etas. (Experiment 16).

Figure 41 shows the total missing neutral mass X in the reaction:

$$\pi^-p \rightarrow \pi^+\pi^-X$$

The large peak centred at the mass of the neutron is from background events of the type:

$$\pi^-p \rightarrow \pi^+\pi^-n$$

which is the largest source of background in the experiment. A cut requiring Mass(X) > 1·2 x Mass (neutron) removes essentially all these unwanted events and the remaining events are from η decays plus some small background.

In figure 42 the mass distribution of the η decays as selected above is shown. The full width at half height of this peak is 4·5 MeV and this is the expected width from the known experimental errors. This width is expected to decrease to 3 MeV when all available information is used. The background level from $\pi^+\pi^-\pi^\circ$ phase space is seen to be small.

Experiment 17

WESTFIELD COLLEGE, LONDON
RUTHERFORD LABORATORY

Search for the Decay $\eta \rightarrow \pi^\circ e^+e^-$

The decay $\eta \rightarrow \pi^\circ e^+e^-$ is essentially forbidden; unless there is a charge conjugation (C) violating component in the electromagnetic interaction this decay is immeasurably rare. The allowed rate has been estimated as being of the order of 10^{-10} of all η decays. No decays of this kind have been observed; the current experimental upper limit is 2×10^{-4} of all η decays. A reliable rate measurement of $\eta \rightarrow \pi^\circ e^+e^-$ is of comparable interest to the charge asymmetry in $\eta \rightarrow \pi^+\pi^-\pi^\circ$ (Experiment 16), and a direct pointer to any C violation taking place through the electromagnetic interaction.

To detect this decay mode of the η, the charge asymmetry experiment described in Experiment 16 is modified by the addition of a large, three element gas Cerenkov counter around the spark chambers. This detects the electrons or positrons from the decay, and the event is labelled accordingly. Data is taken concurrently with the asymmetry experiment.

A rate for this forbidden process comparable with the present upper limit will give about 100 $\eta \rightarrow \pi^\circ e^+e^-$ events in the total data. In addition to these real events about 5 background events will survive the full analysis.

Experiment 18

UNIVERSITY COLLEGE, LONDON
UNIVERSITY OF BRISTOL
UNIVERSITY OF LIVERPOOL
RUTHERFORD LABORATORY

ISR Experiment to Search for the Intermediate Boson (The Muon Experiment)

The CERN intersecting storage rings (ISR) are due to begin operation during 1971. This new facility will enable two beams of 28 GeV protons to make a 'head-on collision' thus allowing the full energy of both protons to be available for the interaction. When an energetic proton hits a stationary target the major part of the energy is used in recoil of the system and only a small fraction of the primary proton energy is available in the centre of momentum for the reaction. The ISR will provide, for pp collisions, a centre of momentum energy equivalent to that obtained from a 1600 GeV conventional accelerator, i.e. it will make available a total c.m. energy of 56 GeV, and will (in principle) allow the production of, hitherto unknown, very massive particles. The major aim of this experiment is to search for the production of one such particle, the so-called intermediate boson.

Figure 43. Schematic diagram of the apparatus to be used for Experiment 18, at the CERN ISR machine.

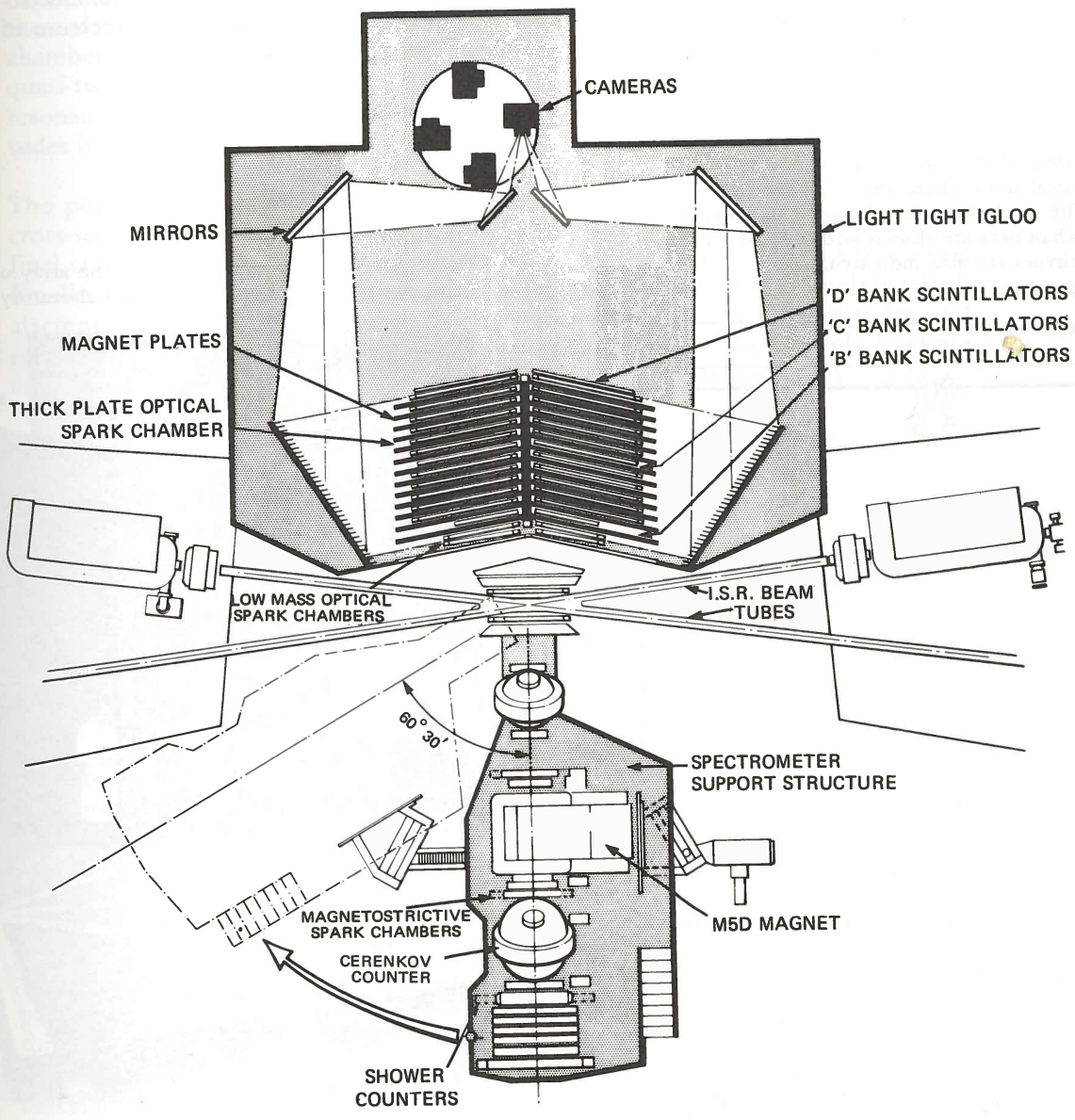

On general grounds any interaction taking place over a finite distance must have some 'messenger' that 'carries' the force between the interacting particles. For the strong interaction there are many 'messengers' (pions, kaons, baryons, etc) and for the electromagnetic interaction the 'messenger' is the photon; but for the weak interaction no particle has been discovered with the required properties. All existing experimental evidence is consistent with the weak interaction having zero range (point interaction) and thus not requiring a 'messenger', but this picture must almost certainly break down at some very short distance. Such a break down would require a large mass 'messenger' known as the 'intermediate boson'. This particle is expected to decay into leptons, e.g.

$$W^{\pm} \rightarrow \mu^{\pm} + \nu_{\mu}$$

If the W particle has a large mass the muons from the decay will have high momentum and can come at large angles from the colliding beams. The present experiment uses a large solid angle array of magnetised iron and optical spark chambers placed at 90° to the colliding beams to identify the muons and measure their momentum (see figure 43). The detector has dimensions 5m x 3m x 4½m (67m³) and weighs ∿ 300 tons (see figures 44 and 45).

The apparatus will also be able to detect pairs of muons produced in electromagnetic interactions from virtual γ-rays and the study of the mass spectrum of these muon pairs is a secondary objective of the experiment.

Figure 44. Front view of the large array of magnetized steel plates and optical spark chambers to be used in Experiment 18. The steel plates are shown with a heavy outline; the spark chambers are shown with dotted outline. The positions of mirrors are also indicated, at 45° underneath the apparatus.

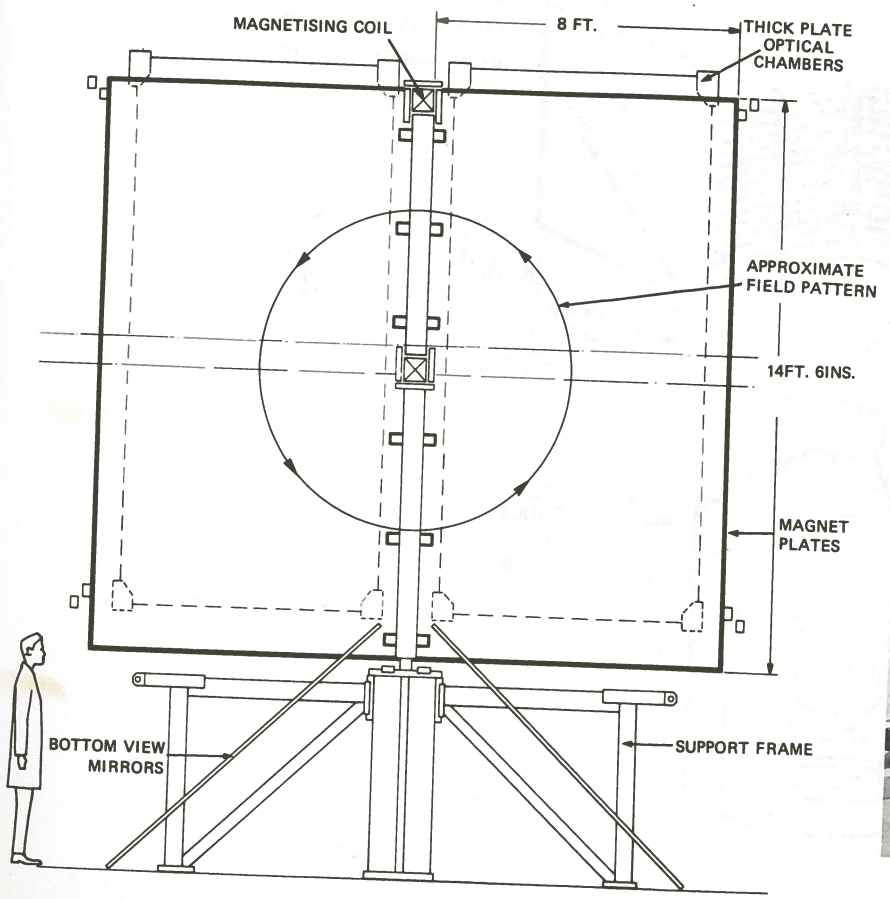

Figure 45. The photograph shows the array of figure 4 being assembled at the Rutherford Laboratory.

A third aim is a measurement of the yield of strongly interacting particles at large angles from the primary p-p interaction. This is of interest in its own right and is also required in the interpretation of the single muon spectrum observed in the search for the W particle. This yield study will be made using the wide angle spectrometer set on the opposite side of the intersection region, as shown in figure 43.

The major parts of both detectors are designed and construction is under way. It is planned to commence installation at the ISR in April 1971 and the experiment is expected to start in June of that year.

CEN, SACLAY.
COLLEGE DE FRANCE
UNIVERSITY OF STRASBOURG
RUTHERFORD LABORATORY

Experiment 19

Formation of Baryon Resonances with Strangeness - 1 in the Mass Range 1915 to 2170 MeV/c² (ref. 10, 11, 71, 86, 87, 88, 89, 99, 105, 106).

K^- mesons incident on protons combine to make composite baryonic states with particular properties of strangeness - 1 and isotopic spin 0 and 1. A resonance is 'formed' when the total energy in the centre of momentum system corresponds to the mass of the resonance. Such states decay by strong interaction (in a time of the order of 10^{-24} sec) into various final states which are observable in a bubble chamber. Of particular interest, because of their simplicity, are the two body and quasi-two body final states. By studying these final states the properties of the resonances such as mass, width, spin, parity, isotopic spin and their decay amplitudes into each final state are derived.

The purpose of the experiment is primarily to make accurate measurements of cross-sections, angular distributions, polarizations and decay distributions of the final states. These data are then analysed to search for known or new resonances. Finally these resonances are examined in relation to theoretical models which attempt to explain the whole spectrum of strongly interacting particles and resonances, and whose validity rests on agreement with the increasingly accurate experimental data. Of particular success is the symmetry scheme SU(3).

In this experiment 1,650,000 pictures of K^-p interactions at 13 energies approximately equally spaced in the interval 1915 to 2170 MeV were taken at Nimrod using the CEN, Saclay, hydrogen bubble chamber. From these pictures approximately 150,000 events have been measured.

The partial wave analyses of the two body final states

$$K^-p \rightarrow \Sigma\pi \quad (1)$$
$$K^-p \rightarrow \Lambda\pi \quad (2)$$
$$K^-p \rightarrow \bar{K}N \quad (3)$$

are now complete. Results for the first two reactions have been published. Reaction (3) has two possible final states $K^-p \rightarrow K^-p$ and $K^-p \rightarrow \bar{K}^\circ n$, called elastic scattering and charge exchange respectively. The latter state is only seen when the K° decays by the K_s° mode into $\pi^+\pi^-$ in the bubble chamber. Figure 46 shows the spectrum of the missing mass squared for all events with just a K_s° decay visible. In this spectrum the $\bar{K}^\circ n$ events are clearly resolved.

The angular and polarization distributions are analysed in terms of amplitudes for partial waves of different angular momentum. In this way resonances of definite spin and parity can be isolated. The results are best displayed by the Argand diagrams of the separate partial wave amplitudes (figure 47). An amplitude which describes an anticlockwise loop with increasing energy in such a diagram may have an associated resonance.

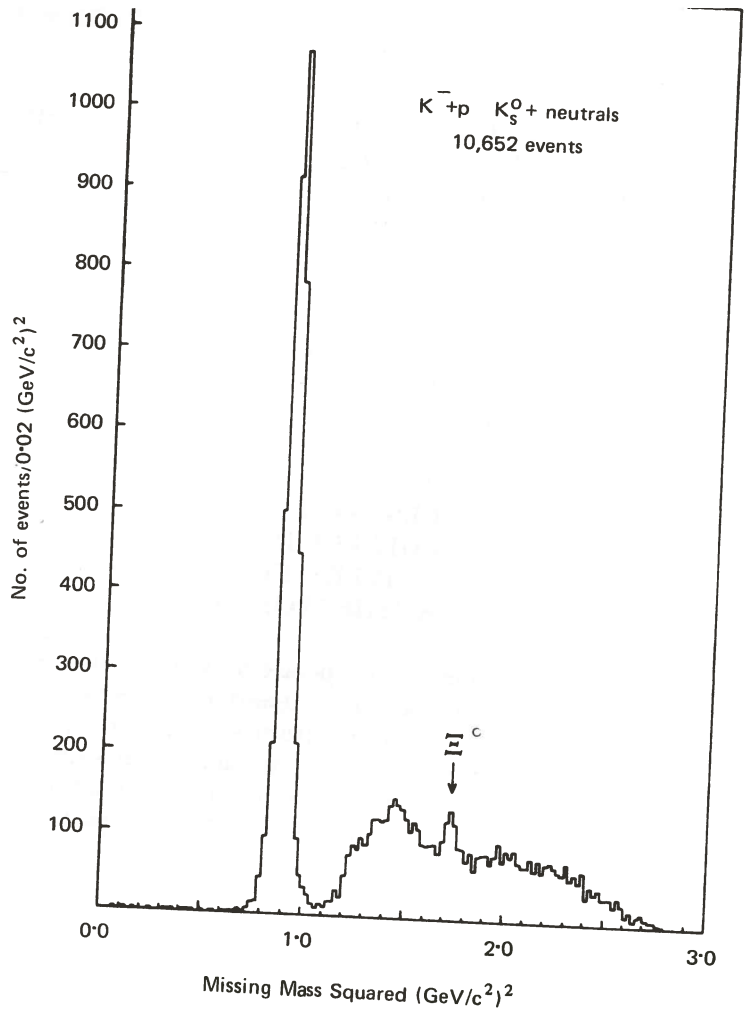

Figure 46. Spectrum of the (missing mass)^2 to the K^0_S in the reaction $K^-p \to K^0_S +$ neutrals for all energies combined. The sharp peak at 0·9 (GeV/c^2)^2 is from the reaction $K^-p \to K^0_S n$. (Experiment 19).

The three dominant resonances in this region are the F_{07} $\Lambda(2100)$, G_{17} $\Sigma(2030)$ and F_{15} $\Sigma(1915)$. The masses, widths and resonant amplitudes in each channel have been measured with the results shown in Table 11. The values are generally in good agreement between the channels except for the width of the $\Lambda(2100)$ which is nearly 3 standard deviations different between the $\Sigma\pi$ and $\bar{K}N$ channels. This problem may be resolved in the study of the other channels in this experiment. The $\Sigma(2030)$ has been placed in an SU(3) decuplet together with the $\Delta(1940)$ and the $\Sigma(1915)$ in an octet with the N(1688) and $\Lambda(1815)$.

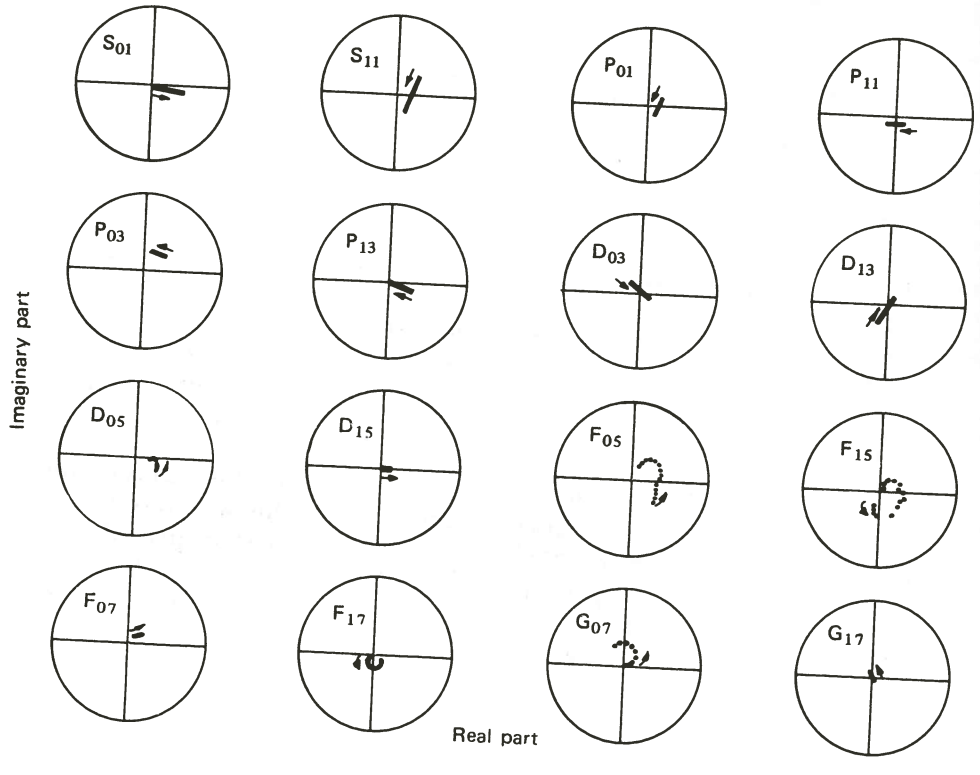

Figure 47(a). Argand diagram for partial waves in the reaction $K^-p \to \Sigma\pi$. Arrows indicate the direction of increasing energy. (Experiment 19).

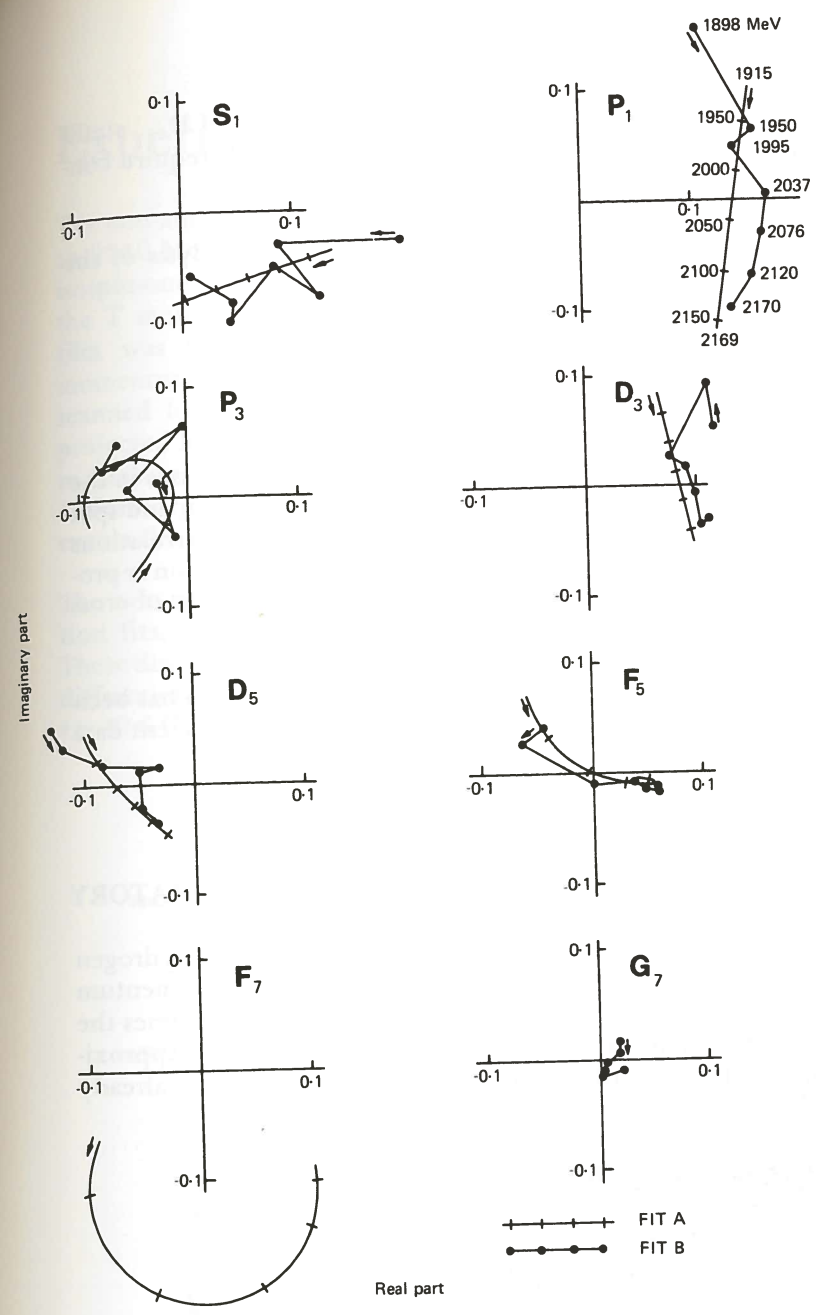

Figure 47(b). Argand diagram for partial waves in the reaction $K^-p \to \Lambda\pi^0$. Arrows indicate the direction of increasing energy. (Experiment 19).

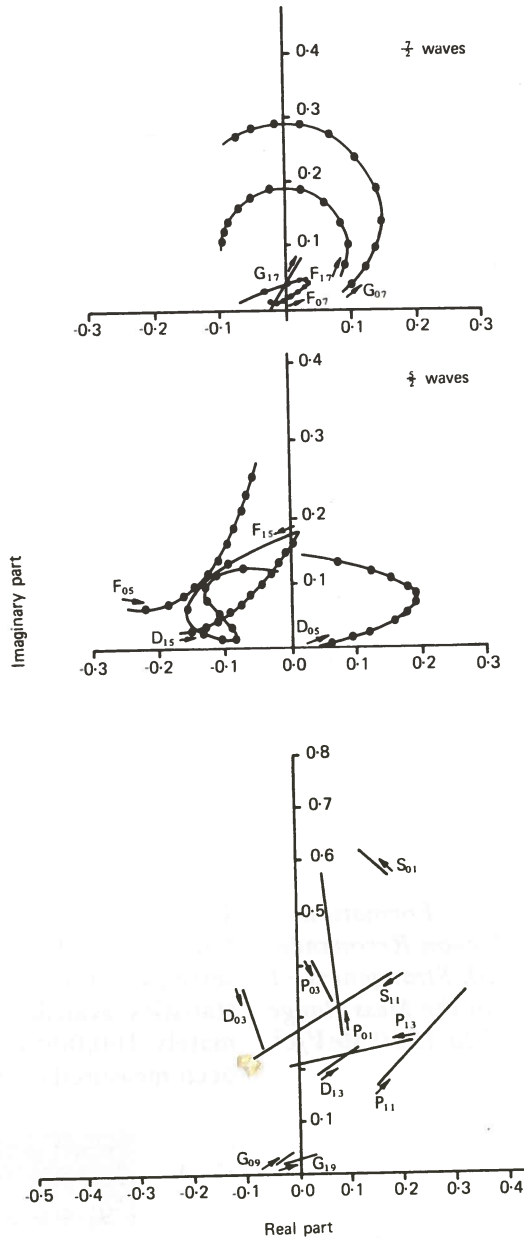

Figure 47(c) Argand diagram for partial waves in the reaction $K^-p \to \bar{K}N$. Arrows indicate the direction of increasing energy. (Experiment 19).

Table 11

Measured parameters of dominant resonances. (Experiment 19).

Resonance	Channel	E_R (MeV)	Γ (MeV)	$\sqrt{xx'}$
$\Sigma(1915)$	$K^-p \to \bar{K}N$	1910 ± 15	70 ± 15	0·15 ± 0·03
	$K^-p \to \Sigma\pi$	1900 ± 15	75 ± 20	−0·13 ± 0·03
	$K^-p \to \Lambda\pi$	1910 ± 20	60 ± 20	0·1 ± 0·02
$\Sigma(2030)$	$K^-p \to \bar{K}N$	2025 ± 15	200 ± 30	0·18 ± 0·02
	$K^-p \to \Sigma\pi$	2030 ± 10	155 ± 20	−0·10 ± 0·03
	$K^-p \to \Lambda\pi$	2030 ± 10	165^{+30}_{-15}	0·2 ± 0·02
$\Lambda(2100)$	$K^-p \to \bar{K}N$	2100 ± 15	300 ± 30	0·30 ± 0·03
	$K^-p \to \Sigma\pi$	2110 ± 30	140 ± 15	0·16 ± 0·02

Several less prominent resonances have been suggested, P_{11}, P_{13} and D_{13} states in the $\Lambda\pi$ analysis and D_{05} and F_{07} states in the $\bar{K}N$, but they all require confirmation from other data.

Quasi-two body final states. Progress is now being made on the analysis of the channels

$$\begin{aligned} K^-p &\rightarrow \Lambda\omega \\ K^-p &\rightarrow Y^*(1385)\pi \\ K^-p &\rightarrow K^*(890)N \end{aligned}$$

Angular and polarization distributions can be obtained for these processes in the same way as for the simple two body channels. The angular distribution and spin orientation of the resonance state are deduced from a study of the correlations between the decay products and the production plane. Further information is provided in the $\Lambda\omega$ channel from an analysis of the Λ decay and the study of cross correlations between this decay and the decay of the ω resonance.

The formalism for a complete partial wave analysis including all this data has been set up and analysis started on the channels. First indications are that sufficient data is available to perform an energy independent analysis.

Experiment 20

RUTHERFORD LABORATORY

Formation of Baryon Resonances with Strangeness -1 in the Mass Range 1775 to 1960 MeV/c²

Film for an extension of Experiment 19 was exposed at CERN in the 2 m hydrogen bubble chamber during April/May 1970. It comprises 11 beam momentum settings in the range 1·0 to 1·4 GeV/c and will provide approximately 4 times the statistics available in any previous experiment in this energy range. Approximately 100,000 events, about one third of the expected final total, have already been measured on the HPD.

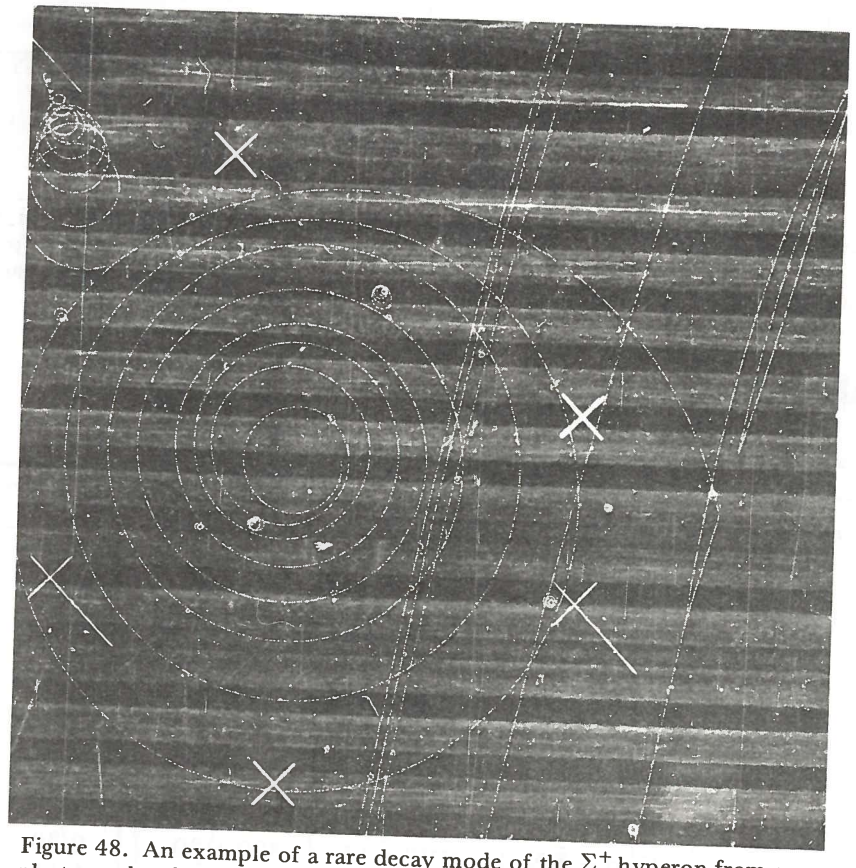

Figure 48. An example of a rare decay mode of the Σ^+ hyperon from a photograph taken in the Saclay 81 cm Bubble Chamber at Nimrod. The reaction is $K^-p \rightarrow \Sigma^+\pi^-$, followed by $\Sigma^+ \rightarrow \Lambda e^+\nu$ and $\Lambda \rightarrow p\pi^-$.

Experiment 21

UNIVERSITY OF LIVERPOOL. RUTHERFORD LABORATORY

Non-Annihilation Channels in $\bar{p}p$ Interactions near C.M. Energy 2200 MeV (ref. 90, 122)

The non-annihilation channels of the $\bar{p}p$ interactions in the C.M. energy range 2150 to 2240 MeV are being studied. This range approximately covers the width of the isospin-one structure seen in the $N\bar{N}$ total cross-section at 2190 MeV, and contains the T meson observed in the CERN missing mass spectrometer experiment. The film was taken using the CERN 2 m bubble chamber with four antiproton momentum settings centred at 1·23, 1·30, 1·36 and 1·43 GeV/c. The film was scanned for two prong events with the requirement that protons should have a projected length greater than 1 mm on the film (14 mm in the chamber). Measurements were made by the HPD and events analysed through the standard Rutherford Laboratory geometry and kinematics programs. After a remeasurement of failed events the data sample consists of 75,000 events.

The non-annihilation events were uniquely identified from kinematic and ionisation fits. The differential cross-sections at all momenta are plotted in figure 49. These distributions exhibit the well known features of $\bar{p}p$ scattering: a large forward diffraction peak, a first minimum at $t \simeq -0{\cdot}4$ GeV^2 and a second maximum at $t \simeq -0{\cdot}6$ GeV^2.

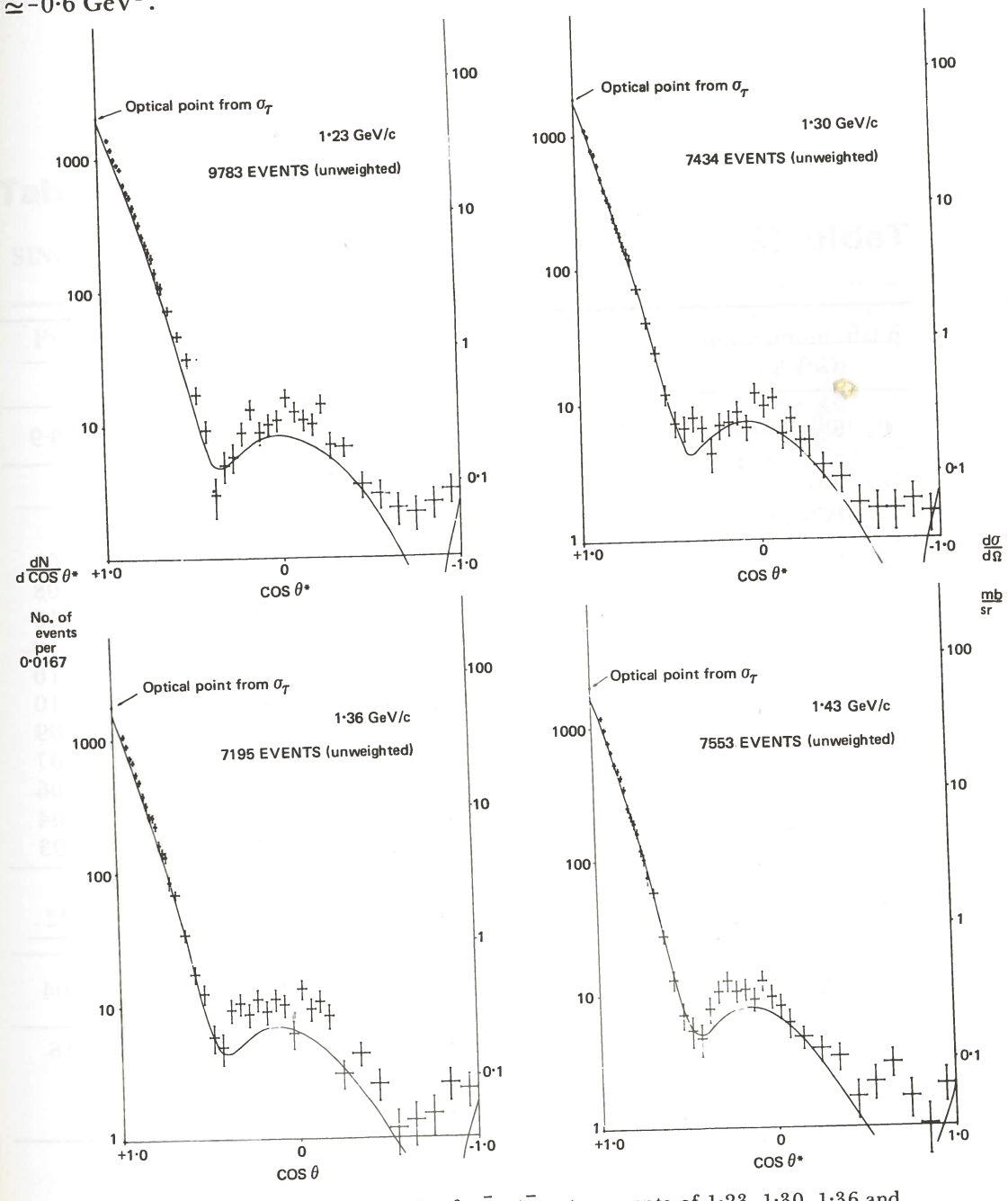

Figure 49. Differential cross-section for $\bar{p}p \rightarrow \bar{p}p$ at momenta of 1·23, 1·30, 1·36 and 1·43 GeV/c. (Experiment 21).

To obtain the total elastic scattering cross-section, the experimental differential cross-section must be extrapolated to t = 0. Since this correction is sizable (about 30%), a variety of feasible extrapolations have been used to investigate the sensitivity of the final result to the choice of functional form. The results quoted in Table 12 have been obtained by extrapolating with a Legendre Polynomial expansion fitted to the experimental centre of momentum angular distributions in the range $-1{\cdot}0 < \cos\theta < +0{\cdot}95$. All of the coefficients are increasing with energy as expected for a diffraction-like distribution exhibiting a forward peak followed by a dip at fixed t. The form $Ae^{bt + ct^2}$ also gives a good fit to the forward peak at all four momenta with $b = 13{\cdot}48 \pm 0{\cdot}33$, $c = 11{\cdot}0 \pm 1{\cdot}3$ and agrees with the Legendre expansion when extrapolated to t = 0.

The ratios of the real to imaginary part of the forward amplitude have been estimated through the optical theorem using the total cross-section data of Abrams et al.; these too are summarized in Table 12. This ratio, averaged over this rather narrow energy range, is found to be $0{\cdot}31 \pm 0{\cdot}04$ which agrees with the theoretical predictions of Soding and of Bryan and Phillips. The possibility of measuring this ratio arises through the capability of the bubble chamber technique to observe small angle scatters.

Table 12

$\bar{p}$ lab. momentum (GeV/c)	1·23	1·30	1·36	1·43
σ_{el} milli-barns	43·3 ± 1·0	41·5 ± 1·0	42·2 ± 0·9	41·8 ± 0·9
Legendre Coefficients				
A_1/A_0	2·58 ± ·06	2·62 ± ·07	2·61 ± ·06	2·65 ± ·05
A_2/A_0	3·40 ± ·09	3·53 ± ·10	3·52 ± ·08	3·63 ± ·08
A_3/A_0	3·41 ± ·11	3·68 ± ·12	3·67 ± ·10	3·91 ± ·10
A_4/A_0	2·77 ± ·11	3·18 ± ·13	3·19 ± ·11	3·54 ± ·10
A_5/A_0	1·79 ± ·11	2·29 ± ·13	2·26 ± ·11	2·73 ± ·10
A_6/A_0	0·95 ± ·11	1·39 ± ·12	1·31 ± ·10	1·80 ± ·10
A_7/A_0	0·43 ± ·10	0·76 ± ·11	0·66 ± ·10	1·05 ± ·09
A_8/A_0	0·16 ± ·08	0·35 ± ·09	0·26 ± ·08	0·59 ± ·07
A_9/A_0	0·01 ± ·07	0·14 ± ·07	0·09 ± ·07	0·32 ± ·06
A_{10}/A_0	-0·02 ± ·04	0·03 ± ·04	0·01 ± ·04	0·16 ± ·04
A_{11}/A_0	-0·02 ± ·03	0·02 ± ·03	0·01 ± ·03	0·06 ± ·03
$\frac{d\sigma(0)}{dt}\left(\frac{mb}{GeV^2}\right)$	626 ± 33	631 ± 31	585 ± 25	61 ± 22
$\left\lvert\frac{\text{Re } f(0)}{\text{Im } f(0)}\right\rvert^2$	0·05 ± ·05	0·09 ± ·05	0·04 ± ·05	0·17 ± ·04
$\frac{d\sigma}{d\Omega}$ (μb/sr) $(-0{\cdot}8 > \cos\theta > -1{\cdot}0)$	108 ± 18	80 ± 17	137 ± 23	71 ± 16

Single Pion Production Channels. The following single pion production reactions have also been studied:

$$\bar{p}p \to \bar{p}p\pi^\circ \quad (1)$$
$$\bar{p}p \to \bar{p}n\pi^+ \quad (2)$$
$$\bar{p}p \to \bar{n}p\pi^- \quad (3)$$

The cross-sections for these three reactions are presented in Table 13. Charge conjugation invariance requires that reactions (2) and (3) should have equal cross-sections and this is satisfied by the data.

Assuming the πN and $\pi\bar{N}$ states are predominantly isospin $\frac{3}{2}$, the following relation between the cross-sections is predicted:

$$\sigma(\bar{p}p\pi^\circ) = \sigma(\bar{n}p\pi^-) + \sigma(\bar{p}n\pi^+)$$

This is indeed found to be the case (see Table 13) within the statistical accuracy of this experiment. Using this result the single pion production cross-sections including the unobserved $\bar{n}n\pi^\circ$ final state can be calculated; these $\bar{N}N\pi$ cross-sections are listed in Table 13.

Table 13

SINGLE PION PRODUCTION CROSS-SECTIONS

Final State	Momentum (GeV/c)	Number of Events	Cross-Section (μb)
$\bar{p}p\,\pi^\circ$	1·23	239	526 ± 35
	1·30	283	739 ± 46
	1·36	383	1011 ± 54
	1·43	513	1247 ± 60
$\bar{p}n\,\pi^+$	1·23	91	200 ± 21
	1·30	107	279 ± 28
	1·36	147	388 ± 33
	1·43	241	586 ± 39
$\bar{n}p\,\pi^-$	1·23	94	207 ± 22
	1·30	136	355 ± 32
	1·36	174	459 ± 36
	1·43	266	646 ± 42
$\bar{N}N\,\pi$	1·23	-	1400 ± 70
	1·30	-	2060 ± 94
	1·36	-	2780 ± 110
	1·43	-	3720 ± 125

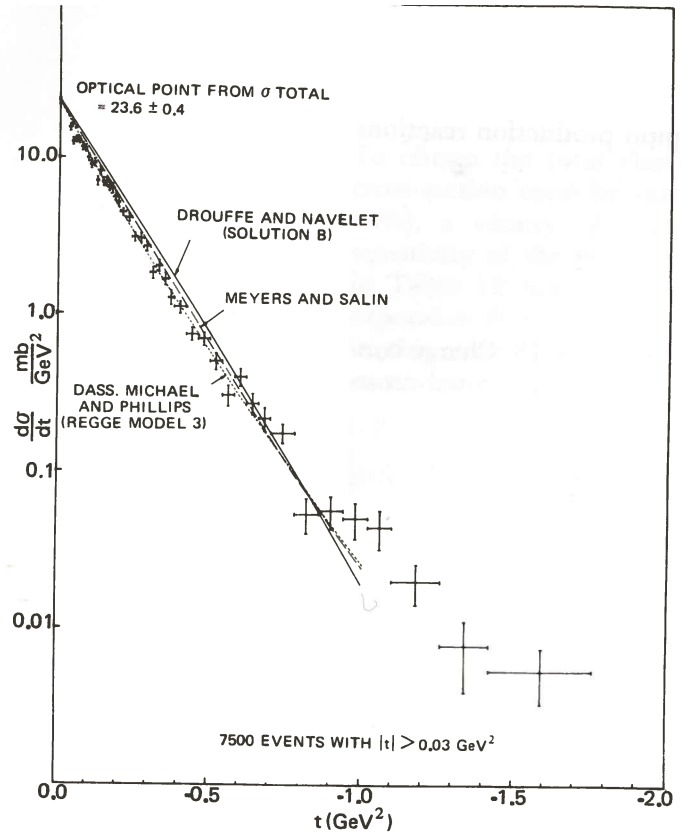

Figure 50. The differential cross-section for K^-p elastic scattering at 14·25 GeV/c. The lines shown with the experimental points are from three Regge pole models. (Experiment 22).

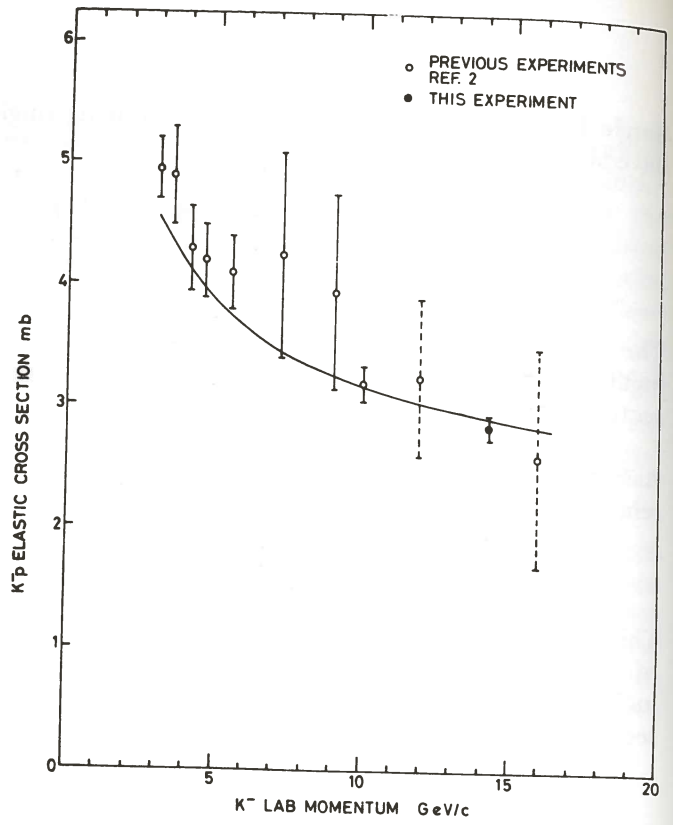

Figure 51. The integrated K^-p elastic cross-sections shown as a function of K^- laboratory momentum. (Experiment 22).

Experiment 22

CEN, SACLAY
ECOLE POLYTECHNIQUE
RUTHERFORD LABORATORY

The Study of 14 GeV/c K^-p Interactions (ref. 100)

The interactions of K^- mesons with protons at 14·25 ± 0·10 GeV/c are being studied. The aim of the experiment is exploratory since this is the highest energy K^- experiment yet attempted. Of particular interest will be the production of strange baryon and meson resonances against a relatively small 'phase space background'.

The film was obtained from CERN using the 2 m hydrogen bubble chamber in the high momentum r.f. separated beam. The first instalment of 350,000 pictures was taken in mid-1969 and measurement of the Rutherford Laboratory's share of the film is essentially complete. A further 400,000 pictures will be taken early in 1971.

First results on K^-p elastic scattering were presented at the 15th International Conference on High Energy Physics in Kiev and will be published soon. Most of these events were measured on the Rutherford Laboratory HPD measuring machine. On high momentum tracks, small residual distortions become as important as other sources of measurement error, and after extensive study, an empirical correction to the geometrical reconstruction was introduced to minimize these effects.

The elastic differential cross-section, corrected for scanning losses, is displayed in figure 50. The integrated elastic cross-section together with the results from other high energy experiments is shown in figure 51. As is readily seen, the present experiment has greatly reduced the error on this cross-section at high energy, emphasizing that the bubble chamber technique can be used efficiently for studying elastic scattering in certain cases.

Physics analysis on the many other reaction channels available in high energy K^-p interactions is now in progress.

Experiment 23

UNIVERSITY OF BIRMINGHAM
UNIVERSITY OF DURHAM
RUTHERFORD LABORATORY

The Study of 4 GeV/c π^+d Interactions

The aim of this experiment is to study the neutral boson states B° produced in the reaction $\pi^+ + d \rightarrow p + p_s + B^\circ$ where p_s is the spectator proton and p is the proton off which B° recoils. Of particular interest is the splitting of the A_2° meson, which is produced with a cross-section $\simeq$ 200 μb in this reaction, and the f° meson ($\sigma \sim$ 100 μb).

The experiment is designed to be of high resolution and high statistics improving on similar previous experiments by a factor $\sim$ 4 in statistics and perhaps 2 in resolution. An exposure of 800,000 pictures, in the CERN 2 m bubble chamber filled with deuterium, has been requested. A total of 421,000 has already been taken.

The film is being scanned and measured simultaneously using the on-line scanning system recently introduced at the Rutherford Laboratory.

Experiment 24

IMPERIAL COLLEGE, LONDON
WESTFIELD COLLEGE, LONDON

π^+p Interactions in the Range 0·8-1·7 GeV/c (ref. 3,131)

This is an experiment to study the formation of baryon resonances with strangeness 0 and isotopic spin $\frac{3}{2}$, called Δ resonances.

(i) **0·9 to 1·05 GeV/c**

Photographs of π^+p interactions at π^+ beam momenta of 0·895, 0·945, 0·995 and 1·040 GeV/c obtained in the Saclay 80 cm chamber at the Rutherford Laboratory have been analysed yielding approximately 55K fitted events. The differential and total elastic scattering cross-sections have been published. The results are in good agreement with previous measurements using counter techniques except at extreme backward angles where significantly lower cross-sections are obtained (figure 52).

Figure 52. The π^+p differential cross-section for backward angles at 0·945 GeV/c (from Experiment 24) compared with the counter data of Duke et al.

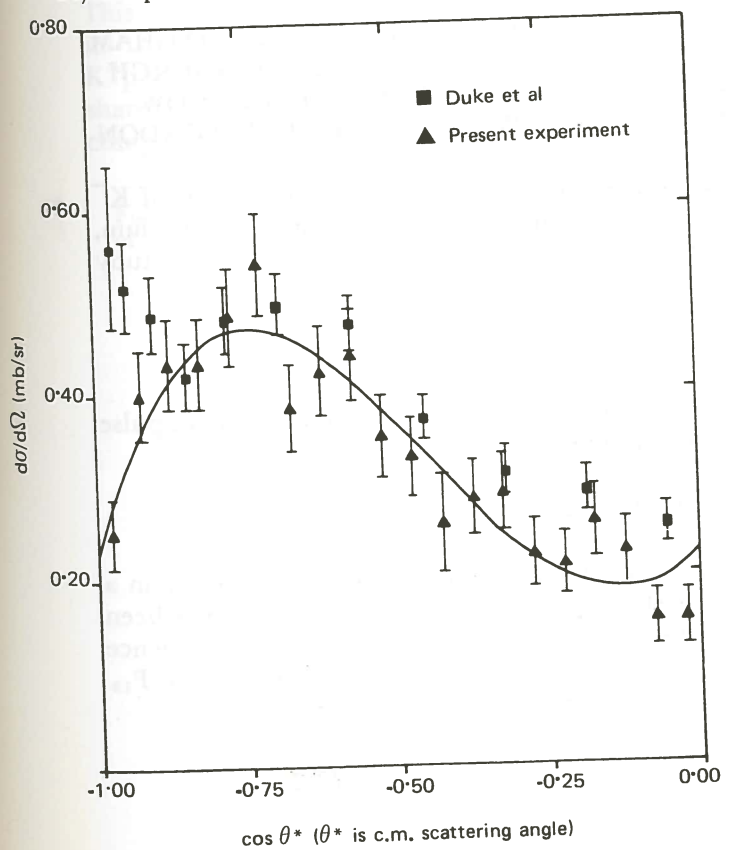

Figure 53. Isobar model fit at 0·995 GeV/c to the mass plots, the Valladas polar and azimuthal angles, Θ and Φ and the centre of momentum production angle of the proton. (Experiment 24).

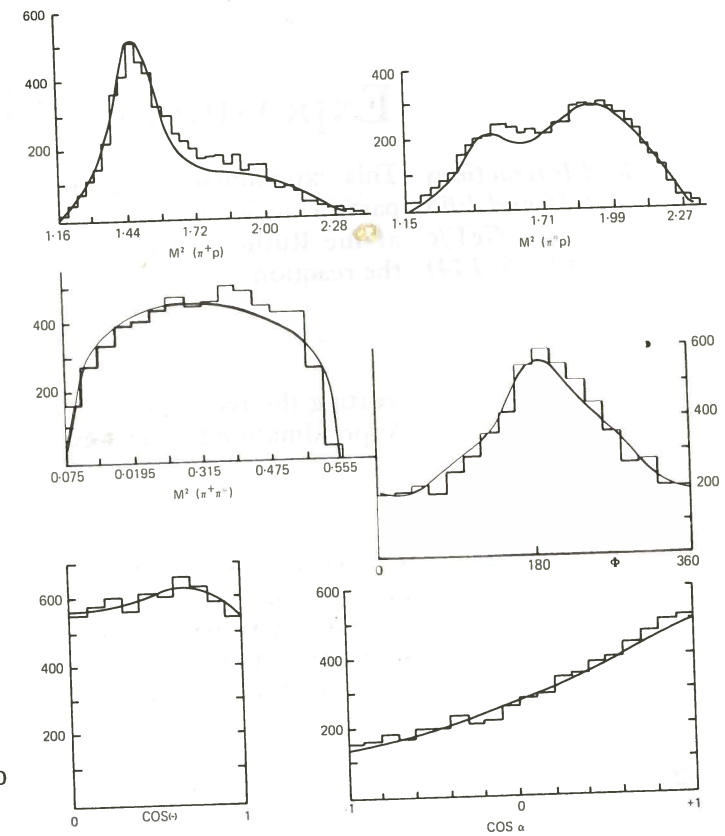

A phase shift analysis on the elastic data has been completed and was presented at the Durham Conference. The analysis shows clearly that the effect of the new data is to select strongly the CERN phase shifts rather than those of Saclay in the D_{33} and D_{35} waves where the two sets of solutions were in greatest disagreement. The only significant departure from the CERN solutions is found in an increased inelasticity of the S-wave.

The inelastic interactions at these momenta have also been fully analysed and papers are in preparation for publication. Partial cross-sections have been obtained and the single pion production is shown to be dominated by production of the $\Delta(1238)$. A detailed study of the short-comings of simple production models using the high statistics available has now been completed. A partial wave analysis of the inelastic scattering in terms of $\pi\Delta$ production has been made. It shows remarkable agreement with the incident partial wave inelasticities of the CERN phase shift solutions. Only the S-wave requires a contribution from production processes other than $\pi\Delta$. This together with the increased inelasticity required by the elastic partial wave analysis indicates the need for strong S-wave contributions from other inelastic channels such as ρN or πN^* even at these low momenta. Figure 53 shows an isobar model fit to the data at 0·995 GeV/c.

(ii) 1·1 to 1·7 GeV/c

The Cambridge film analysis group has joined Imperial College and Westfield College in the analysis of 200K pictures of π^+p interactions obtained from the 1·5 m hydrogen bubble chamber at the Rutherford Laboratory. The film at 1·1 GeV/c has been conventionally measured and that at 1·2 and 1·3 GeV/c has been measured on the Imperial College HPD.

(iii) 0·8 to 1·25 GeV/c

To complete the study at momenta around 1 GeV/c and investigate further the results reported in (i) above, 30K pictures were taken at each of four momenta 0·8, 0·85, 1·15 and 1·25 GeV/c in the 1·5 m hydrogen bubble chamber.

Experiment 25

UNIVERSITY OF BIRMINGHAM
UNIVERSITY OF EDINBURGH
UNIVERSITY OF GLASGOW
IMPERIAL COLLEGE, LONDON

K^-d Interactions at 1·45 and 1·65 GeV/c (ref. 14, 18, 134)

This experiment was performed using an electrostatically separated beam of K^- particles incident on the Saclay 80 cm bubble chamber, filled with liquid deuterium, at the Rutherford Laboratory. The main purpose of this experiment is to study the reaction

$$K^-d \rightarrow \Lambda\pi^-p \qquad (1)$$

treating the recoil proton from the deuteron as a spectator and using the Impulse Approximation to select events corresponding to

$$K^-n \rightarrow \Lambda\pi^- \qquad (2)$$

This channel is important since it selects baryon states with strangeness -1 in a pure isotopic spin state, I = 1. A partial wave analysis on this reaction has been carried out in which the parameters of the $\Sigma(2030)$ were determined; evidence supporting the existence of an $\Sigma(1915)$ F_{15}, and new evidence for a P_{13} resonance with a mass of 2080 MeV/c^2 was found.

As a by-product of this work a sample of events of type (1) where the proton could not be treated as a spectator was obtained. In this sample there is a sharp peak in the Λp effective mass distribution at the position of the Σn threshold, confirming results found in K^-d interactions from 0 to 1 GeV/c. The data is consistent with either a Λp resonance at 2130 MeV or with a threshold effect in the Σn system leading to Λp via the sequence

$$K^-d \rightarrow \Sigma^+\pi^-n,$$
$$\Sigma^+n \rightarrow \Lambda p$$

Elastic scattering, $K^-n \rightarrow K^-n$, has also been analysed in terms of partial waves. The elasticity of the $\Sigma(2030)$ was found to be 17%. Some work on other final states produced by K^-n interactions is in progress. In particular branching fractions of $\Sigma(1385)$ and $\Lambda(1520)$ are being determined and the general characteristics of Y* production processes are being studied.

Experiment 26

CEN, SACLAY
IMPERIAL COLLEGE, LONDON
WESTFIELD COLLEGE, LONDON } K^+p

IMPERIAL COLLEGE, LONDON
WESTFIELD COLLEGE, LONDON } K^+d

K^+N Interactions in the 2 to 3 GeV/c Region

K^+N interactions are of interest because of their relevance to the Simple Quark Model of elementary particles. So far all of the observed experimental resonance spectrum is accommodated in this model, in which baryon states are composed of three quarks. Other possible baryon states which can be constructed using a larger number of quarks are termed 'exotic'.

The search for exotic states is therefore of great importance. One particular such state is the baryon with strangeness +1 called Z*, which, in principle, can be formed in K^+N interactions. Peaks have been seen in K^+N total cross-sections and several experiments have been set up to investigate the nature of these 'bumps'.

This experiment is a survey of K^+p and K^+d interactions in the 2-3 GeV/c region. This energy was chosen because it covers the position of the third 'Cool bump' in the total cross-sections. All events from the 200,000 photographs of the K^+p interactions have been analysed. The Imperial College and Westfield College share were measured on the Imperial College HPD. This is therefore the first completed experiment using that device.

Figure 54. Legendre polynomial coefficients for the reaction $K^+p \rightarrow K^{*+}p$ as a function of the kaon laboratory momentum. (Experiment 26).

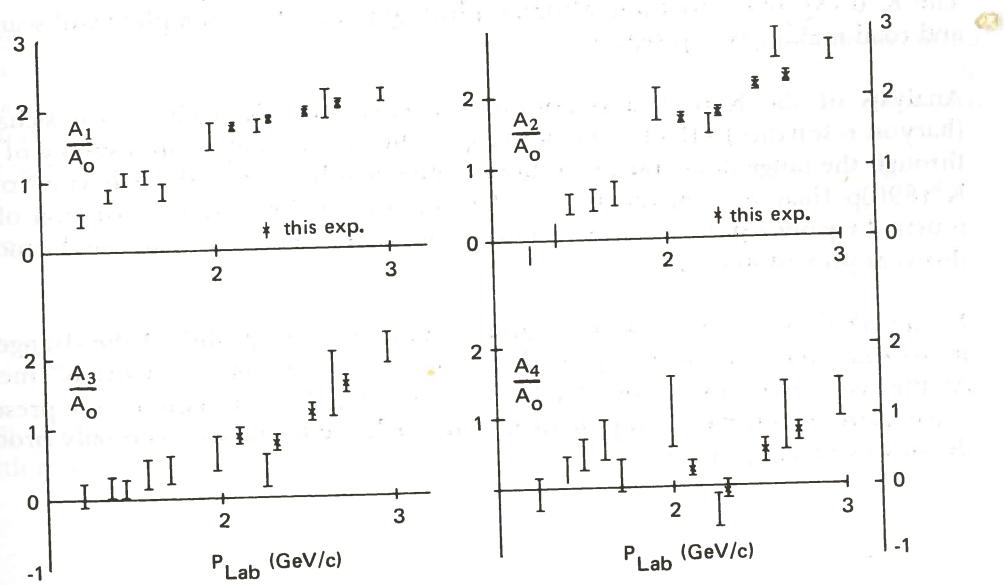

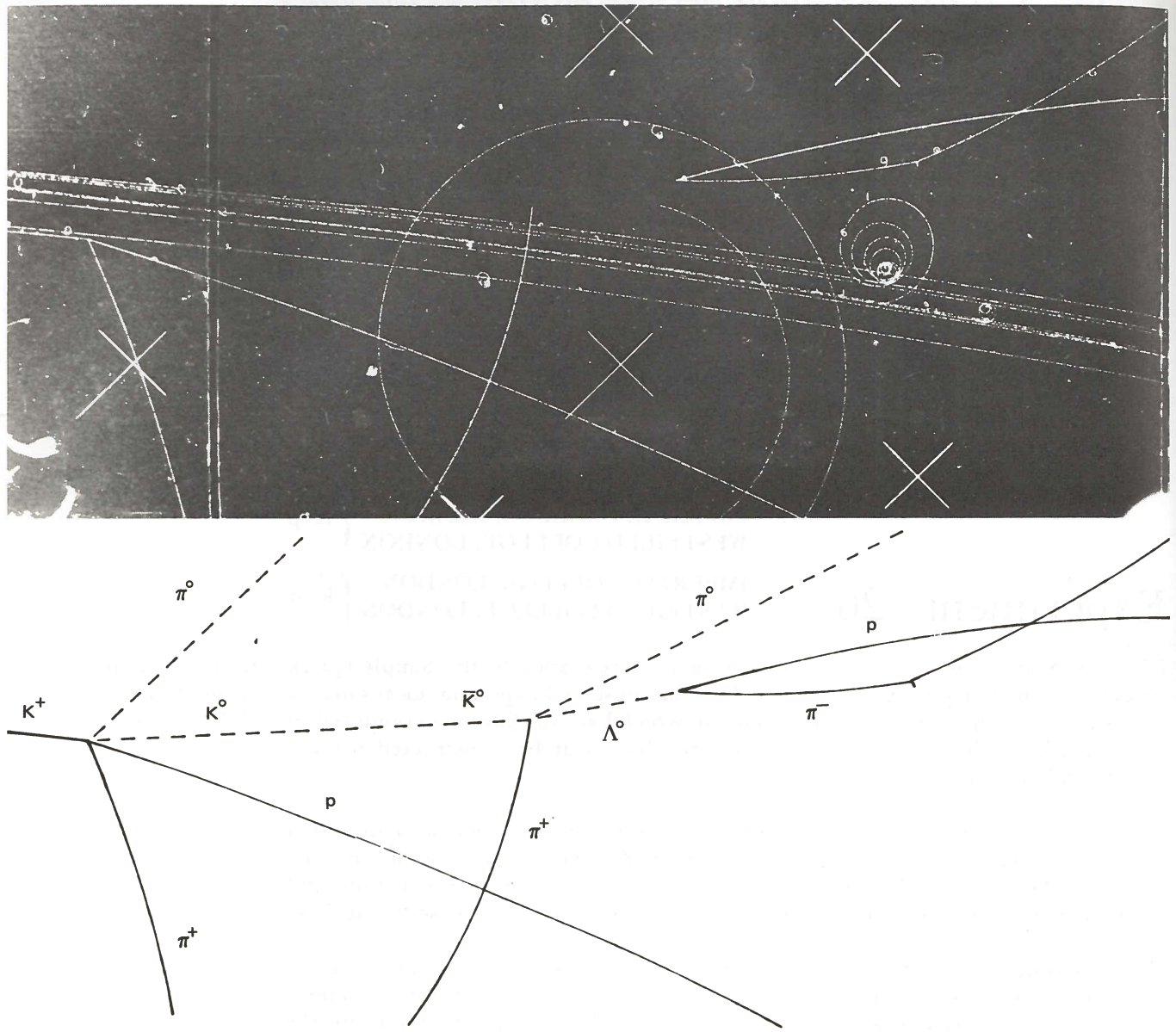

Figure 55. An event taken from K^+p film which displays the $K^\circ \rightarrow \bar{K}^\circ$ transition. (Experiment 26).

The K^+d exposure, totalling 800,000 photographs, is now complete and scanning and road-making is in progress.

Analysis of the K^+p data is continuing. There is little evidence for s-channel (baryon resonance) effects contributing to the 'Cool bump', but a survey of data through the range does appear to show some perturbations in the behaviour of the K*(890)p final state in this region. An example of this is the fluctuation of the fourth Legendre polynomial coefficient shown in figure 54. The significance of this is at present unclear.

Figure 55 shows an interesting example, found in the K^+p film, of the strangeness transformation accompanying the decay of the K°_s component of the K° meson. At the secondary interaction a Λ hyperon is created which required the presence of a negative strangeness component $\bar{K}^\circ$, although the K^+ mesons can only produce the positive strangeness K°.

Experiment 27

UNIVERSITY OF CAMBRIDGE

n-p Interactions from 1 to 7·5 GeV/c (ref. 129, 133, 137)

Neutron-Proton interactions are being studied from an exposure of 112,000 pictures in the 1·5 m hydrogen bubble chamber. A 8·3 GeV/c extracted proton beam incident on a Be target, approximately 7·8 metres from the chamber, was used to produce the neutron beam.

The final analysis of the following processes is now taking place (including data from an earlier test run of 40,000 pictures):

(a) Single and Multiple Pion Production

$$\begin{aligned} np &\rightarrow pp\pi^- \\ &\rightarrow pp\pi^+\pi^-\pi^- \\ &\rightarrow pp\pi^+\pi^+\pi^-\pi^-\pi^- \end{aligned}$$

(b) Strange Particle Production

$$\begin{aligned} np &\rightarrow \Lambda p\, K^\circ \text{ and } \Sigma^\circ p K^\circ \\ &\rightarrow \Sigma^- p\, K^+ \\ &\rightarrow \Lambda p\, K^+\pi^- \text{ and } \Sigma^\circ p\, K^+\pi^- \\ &\rightarrow \Sigma^- p\, K^\circ \pi^+ \end{aligned}$$

Experiment 28

UNIVERSITY OF CAMBRIDGE

n-p Interactions from 1 to 3·5 GeV/c

About 90,000 pictures containing on average two 3-prong events per picture were taken in the 1·5 m hydrogen bubble chamber in November 1970 using an improved design of neutron beam. The neutrons are contained within a band 2 cm wide.

It is proposed to study the following processes with high statistics:

$$\begin{aligned} np &\rightarrow pp\pi^- \\ &\rightarrow pp\pi^-\pi^\circ \\ &\rightarrow pn\pi^+\pi^- \end{aligned}$$

These account for about 75% of the 3-prong events. Approximately 40% of the observed 3-prong events are expected to be $np \rightarrow pn\pi^+\pi^-$ and higher momentum data suggest that at least one half of the events in this channel can be explained in terms of the process $np \rightarrow \Delta^-(1236)\,\Delta^{++}(1236)$, the Δ^- being associated with the neutron vertex.

The strange particle production processes

$$\begin{aligned} np &\rightarrow \Lambda p K^\circ \text{ and } \Sigma^\circ p K^\circ \\ &\rightarrow \Sigma^- p K^+ \end{aligned}$$

will also be studied chiefly with a view to observing the variation of cross-section with momentum near threshold.

Experiment 29

UNIVERSITY COLLEGE, LONDON
TUFTS UNIVERSITY, USA
UNIVERSITY OF BRUSSELS
CERN

K^- Interactions at a Momentum of 2·2 GeV/c in the 1·4 m Heavy Liquid Bubble Chamber (ref. 41)

The heavy liquid bubble chamber is particularly useful for the detection of electromagnetic processes because of its high γ-ray conversion efficiency, i.e. $\gamma \rightarrow e^+e^-$, the electron pairs being visible in the chamber; interactions involving the production of π°s can also be detected, since $\pi^\circ \rightarrow \gamma + \gamma$. By using a beam of K^- mesons, particles and resonances with strangeness -1 and -2 which under-go radiative decay can be studied.

For this experiment the chamber was filled with a propane-freon mixture with average γ-ray conversion efficiency of 55%.

The main aims are:

(i) to find the lifetime of the Ξ° by a method which uses the γ-rays from the Ξ° decay π° to fix the decay point.

(ii) to study the Λ - Λ interaction and the properties of the Ξ^- and Ξ^* resonances.

(iii) to search for X° and ϕ neutral decays and radiative Y* decays.

One publication has now been produced from this experiment and two other pieces of work are nearing completion.

A Russian group had reported a new particle with a mass of 1327 MeV/c^2 which they had observed in the $\Lambda\gamma$ invariant mass spectrum in associated production events with a pion beam in a propane chamber. A scan on 20% of our film by three of the collaborating laboratories has shown that if such a state exists its cross-section for production by K^- collisions on nucleons at 2·2 GeV/c is much less than 100 μb.

The sample of events for our Ξ° lifetime measurement has now been scanned and measured completely. Background studies and tuning-up of the maximum likelihood programs are in progress. Three such programs have been written independently by different collaborators, and a calibration study on Ξ will be carried out as well as the Ξ° measurement.

Over 400 events with two Λ hyperons and an associated K^+ or K° have been measured. Preliminary analysis confirms earlier results that the $\Lambda\Lambda$ mass spectrum peaks strongly close to the threshold. The statistics are large enough for a decay-correlation analysis to be carried out. This will show whether an appreciable part of the low mass $\Lambda\Lambda$ spectrum is contributed by an S-wave interaction between Λ's from the same point in the nucleus.

Experiment 30

UNIVERSITY OF CAMBRIDGE

Anomalies in Electromagnetic Processes (ref. 65, 66, 125)

In a pilot experiment, using the 1·5 m hydrogen bubble chamber, anomalies were found in the distributions of the following three quantities.

(i) Pair α-Anomaly

α is defined as $(p_+ - p_-)/(p_+ + p_-)$ where p_+ and p_- are the momenta of the positive and negative tracks of the pairs which were produced by gamma rays originating in the chamber beam entry windows where incident 1 GeV/c electrons suffered energy losses.

(ii) Pair Energy Anomaly

Writing $k = p_+ + p_-$ and E_o for the incoming beam momentum an enhancement in the distribution of the ratio k/E_o was found at values around 0·83.

(iii) Bremsstrahlung Anomaly

A plot of the ratio of final to initial momentum of 1 GeV/c electrons suffering energy losses in the hydrogen bubble chamber showed an enhancement in the range 0·16 to 0·22.

About 250,000 pictures from a variety of production conditions were taken in April 1970 with a view to studying these processes with much better statistics. Analysis and measurement is still in progress.

Experiment 31

UNIVERSITY COLLEGE, LONDON
CERN
RUTHERFORD LABORATORY

Development of the Neon-Hydrogen Track Sensitive Target Facility

The track sensitive target facility combines the advantages of the hydrogen bubble chamber with those of the heavy liquid chamber. Beam particle interactions occur in a region of pure hydrogen so that the advantages of interaction with a free proton and simple production kinematics are preserved. The hydrogen is contained in a perspex bag within the main chamber which is filled with a heavy liquid mixture of neon and hydrogen. This heavy liquid is efficient for the detection of gamma rays arising from the decay of π°, η° and Σ° particles produced in the target. Operating conditions can be achieved where both the hydrogen and the neon-hydrogen mixture are simultaneously sensitive.

Work has continued during 1970 on the development of this facility in the 1·5m chamber. In collaboration with the operations group the filling problems associated with neon-hydrogen mixtures in the range 35 to 50 mole percent neon have been investigated. Using 700 MeV/c to 780 MeV/c protons which stop in the mixture and the range momentum relationship, it has been shown that the density of the mixture in the chamber agrees with that predicted from the filling technique. This has been checked by comparing the energy loss in the liquid with that in a known thickness of aluminium absorber placed in front of the chamber. Furthermore by measuring the range as a function of beam height in the chamber it has been shown that a uniform mixture with a variation of less than ±½% is obtained.

Because of the development work necessary it was not possible to take physics pictures for Proposal No. 66 during the year. This proposal was to use the heavy liquid as an electron detector to allow the study of the leptonic decays of polarized Λ hyperons produced by 1·040 GeV/c π^- interactions on hydrogen in the target. During 1970 however the CERN spark chamber group has analysed a large number of $\Lambda\beta$-decay events using a different technique so that, in view of the delay in starting physics with the target. Proposal No. 66 has been withdrawn.

It is now proposed to start the physics programme using the target in 1971 with a study of 4 GeV/c π^+p interactions to complement the 4 GeV/c π^+d experiment in progress. This proposal should yield data on the A_2 and H mesons in particular.

Experiment 32

UNIVERSITY OF BIRMINGHAM
UNIVERSITY OF SURREY
RUTHERFORD LABORATORY

Total Reaction Cross-Sections for Pions on Nuclei

This is believed to be the first experiment to be carried out on Nimrod with the object of gaining information about the properties and structure of atomic nuclei rather than the properties and interactions of elementary particles.

The experiment, which is currently in the final stages of setting up and testing of apparatus, is to measure the total reaction cross-sections for π^+ and π^- mesons on a range of nuclei at energies in the region between 0·5 and 2·0 GeV. The eventual aim of these measurements is to obtain further information about the density distribution of neutrons in nuclei, a currently controversial topic in nuclear structure physics.

In heavy nuclei both π^+ and π^- mesons are strongly absorbed in the nuclear interior. However, if for the pion – nucleon total reaction cross-sections (σ_R), the ratio:

$\frac{\sigma_R(\pi^-p)}{\sigma_R(\pi^+p)} = \frac{\sigma_R(\pi^+n)}{\sigma_R(\pi^-n)}$ is much greater than 1 then in the surface region the π^+ will be mainly absorbed by neutrons and the π^- by protons. Hence the ratio of the total reaction cross-sections for pion – nucleus interactions $R = \frac{\sigma_R(\pi^+N)}{\sigma_R(\pi^-N)}$ will be sensitive to the properties of the surface region around the 50% density point and in particular to the relative distributions of neutrons and protons. The ratio R has been measured before for 700 MeV π^+ and π^- mesons, giving R = 2·6, but the measurement was only made for lead and at one pion energy. In the present experiment these measurements will be repeated and extended to cover both a wide range of nuclei and a number of pion energies.

The experiment is being set up in a slightly modified version of the K8 beam line now designated π10. A DISC Cerenkov counter is used to distinguish between protons and π^+ mesons and a threshold Cerenkov counter used to reject electrons and muons. The latter counter will also be used to measure the pion beam momenta. The experiment itself (figure 56) consists of a 'bad-geometry' transmission measurement in which the number of particles transmitted through the target is measured as a function of the solid angle subtended by the elements of an array of scintillation counters. Problems have arisen in previous transmission counter arrays due to the detection of charged particles by Cerenkov light emitted in the plastic light-guides between the scintillators and associated photomultipliers. The present design, which is described in more detail in the instrumentation section, uses air light guides and a carefully chosen geometry which gives a detection efficiency of greater than 99·95% over the surface of the scintillator and to within 1 mm of the edge.

The scalers will be interfaced using the CAMAC system to a PDP-8 computer which will be used for on-line checking of the results. It is hoped to start data taking in the first quarter of 1971.

This experiment is also being carried out in close collaboration with the theoretical nuclear physics group at the University of Surrey who have written the computer programmes which will be required to interpret the results in terms of neutron density distributions. This group has also very fully investigated the theoretical justification for this experiment and several of the corrections which have to be applied to the simplified theory to take into account the Fermi momenta and correlations of the nucleons in the nucleus.

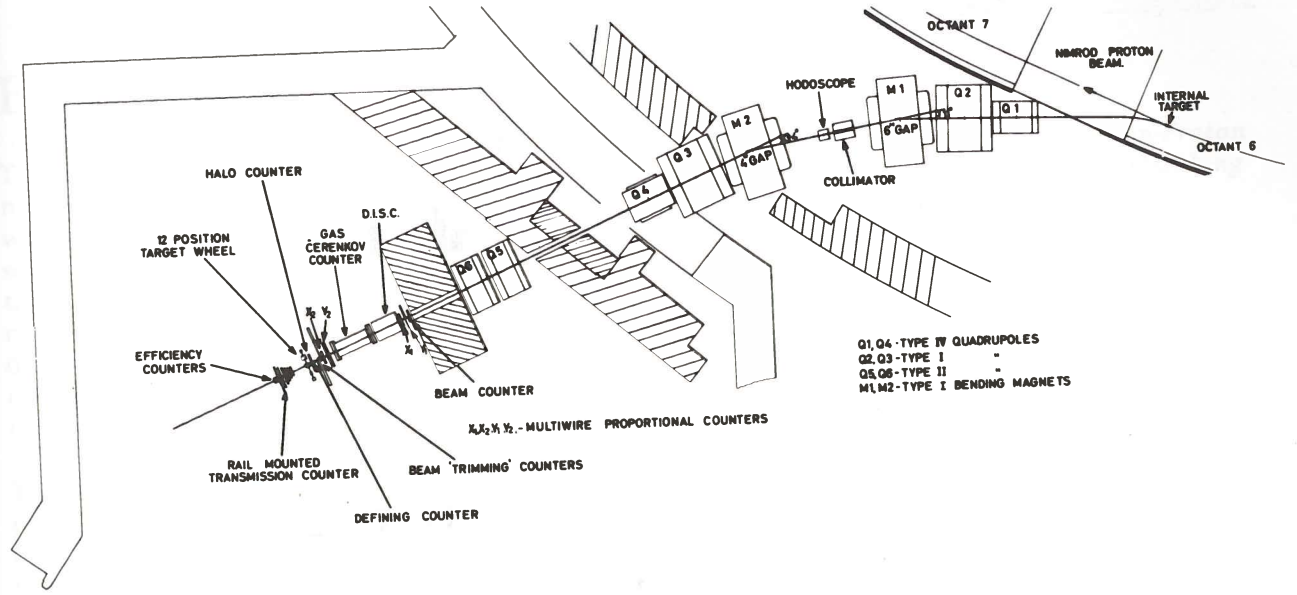

Figure 56. A schematic diagram of the π10 beam-line in Hall 2 and the apparatus used in the nuclear structure experiment on Nimrod. (Experiment 32).

Experiment 33

UNIV. RES. REACTOR, RISLEY
UNIVERSITY OF MANCHESTER
RUTHERFORD LABORATORY

A Search for Super-heavy Elements (ref. 82)

The possible existence of long lived super-heavy nuclei due to the formation of a closed shell of protons at Z = 114 and a closed shell of neutrons at N = 184 has recently been the topic of much theoretical speculation. For some super-heavy nuclei half-lives of as long as 10^8 years have been predicted.

Probably one of the best methods of producing these new elements, if they exist, would be to bombard a heavy element target with a beam of very heavy ions having an energy above that of the Coulomb barrier which exists between the target nuclei and the projectile. At present there are few, if any, accelerators giving directly very heavy-ion beams of sufficient energy.

In the present experiment an attempt has been made to produce super-heavy elements by using secondary reactions in targets irradiated by very high energy protons. For example when 24 GeV protons are elastically scattered from tungsten nuclei at angles greater than 45° the recoil nuclei will have energies greater than the 1·0 GeV Coulomb barrier which exists between two tungsten nuclei. Inelastic reactions may also give fast recoil nuclei. Super-heavy elements could perhaps then be produced as a result of an interaction between a recoiling nucleus and another heavy nucleus in the target.

In order to identify the super-heavy nuclei and to separate them from the other material present in the target it is necessary to rely on the predictions that elements 110, 111, 112, 113 and 114 will be the chemical homologues of Pt, Au, Hg, Tl and Pb respectively. Measurements of the alpha and spontaneous fission activity from the separated sources can then be made to try to identify the possible existence of super-heavy elements.

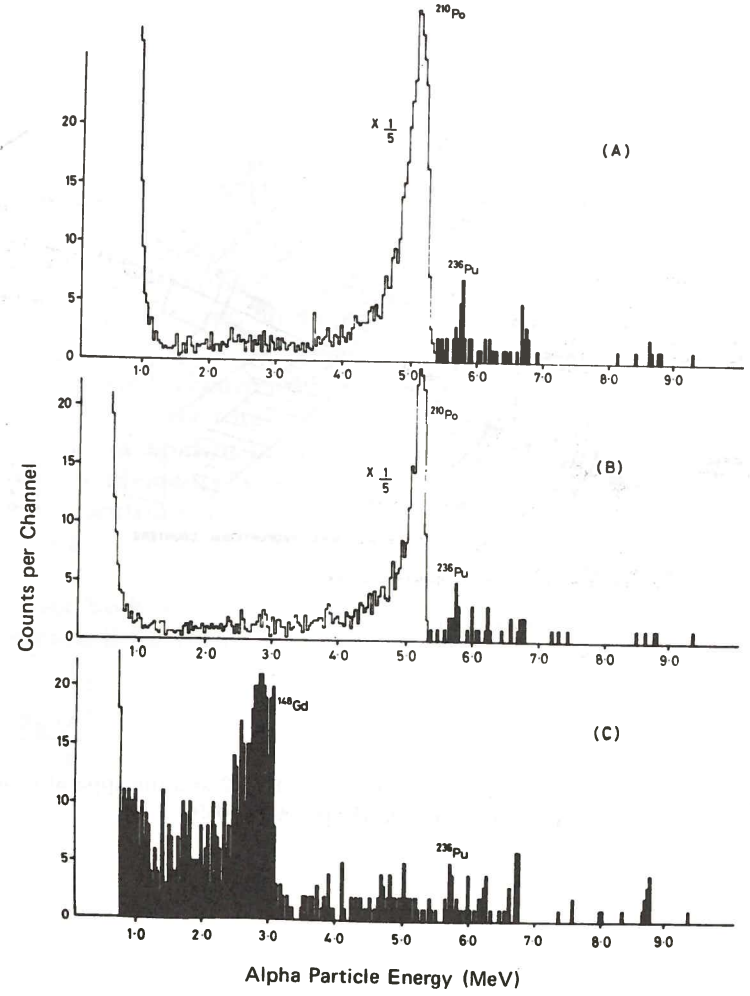

Figure 57. Alpha particle spectra measured with the Hg sources from Experiment 32. Figure (A) and (B) were obtained over periods of 406 and 236 hours respectively with the source obtained from the second tungsten target. Figure (C) was ontained over a period of 280 hours with the source from the first tungsten target.

Three cylindrical tungsten targets have been obtained after each has been irradiated by about 2×10^{18} protons of 24 GeV energy in one of the extracted beams from the CERN Proton Synchrotron. After chemical separation, measurements were then made on Pt, Au, Hg, T1 and Pb sources prepared from these targets.

The most interesting results to date have come from the Hg sources. Clear evidence for spontaneous fission activity has been obtained from the source prepared from the second tungsten target and preliminary measurements on the third target have given encouraging results. It does not seem likely that the observed activity is due to a contaminant. The first target does not seem to show any evidence for spontaneous fission – this may perhaps be due to the source thickness or to the fact that the target is considerably older than the other two.

In measurements of the alpha particle spectra from both the first and second source there is evidence for a group of alpha particles having an energy of 6·75 MeV (figure 57A, B and C). Again, although with less certainty in this case, it is believed that the observed alpha particles are unlikely to be due to any contaminant. The energy of 6·73 MeV is also in good agreement with several predictions for element 112, the homologue of Hg.

Other experiments to try to confirm the above results, and to endeavour to measure either the Z or the A of the decaying nucleus are in preparation. Measurements are also in progress on the other sources (Pt, Au, Tl and Pb) together with investigations of actinide elements which may also be produced in the tungsten targets.

Experiment 34

QUEEN MARY COLLEGE, LONDON
AERE, HARWELL
RUTHERFORD LABORATORY

Neutron-Proton Bremsstrahlung

The purpose of this experiment is to study the bremsstrahlung reaction $n+p \rightarrow n+p+\gamma$ in order to learn about the nucleon-nucleon interaction in conditions where the initial and final state energies of the two nucleons are not the same, the so-called 'off-the-energy-shell' elements of the two nucleon interaction. Calculations of the cross-section for this reaction using different parameterizations of the nucleon-nucleon interaction, which fit the elastic scattering equally well, show different predictions for the bremsstrahlung cross-section. A precise measurement of the npγ cross-section will therefore differentiate between the various nucleon-nucleon potentials currently in use.

The plan of the experiment is shown in figure 58. A neutron beam is produced by peeling off the proton beam from the AERE 110 in synchro-cyclotron onto a beryllium target. The neutron beam is collimated and allowed to strike a liquid hydrogen target. An event is defined by coincidence between a neutron and proton arm on opposite sides of the beam at non conjugate angles, i.e. $\bar{B}(P_1\ P_2\ P_3)_i\ (\bar{N}\nu N)$. Proton arms were at 20°, 32°, and the neutron arms at 23°, 26°, 29° and 38° on both sides of the beam. For each event several parameters are measured including the incident time-of-flight of the neutron, the pulse height recorded in P_3 which gives the proton energy, the time-of-flight of the final state neutron, and the proton time-of-flight between P_1 and P_2. This information, plus identification of the proton and neutron arm which fired, is read into a DDP-516 computer via a CAMAC interface and stored on magnetic tape for later analysis.

With this system data taking has been completed for the npγ experiment and is presently being analysed. Initial setting up for this experiment included a precision measurement of the n-p elastic scattering cross-section for neutrons of 130 MeV. These data have now been analysed and the relative cross-section is compared with previous measurements in figure 59. The relative accuracy for our measurements is 3·5%.

With only slight modifications in the experimental set-up data has been taken for the elastic neutron scattering from deuterium and a kinematically complete experiment on the reaction d(n, np)n is in progress.

Fig. 58. Schematic diagram of the apparatus used in Experiment 34, to study $n+p \rightarrow n+p+\gamma$.

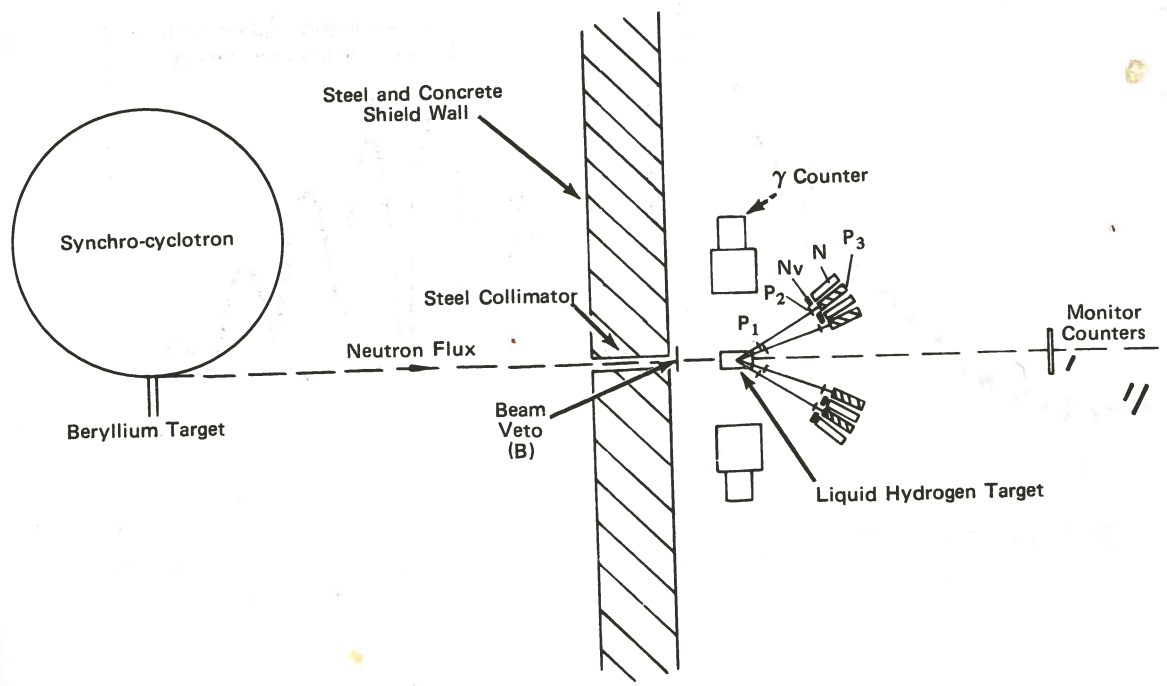

Experiment 35

KING'S COLLEGE, LONDON
WEST HAM COLLEGE OF TECHNOLOGY
UNIVERSITY OF BIRMINGHAM
UNIVERSITY OF KENT

Medium Energy Nuclear Reaction Studies

The backward angle data measured on the Proton Linear Accelerator (PLA), for the scattering of 50 MeV protons from Be, C, N and O nuclei have been analysed using the simple Optical Model. An improvement in the quality of the fits and better systematics in the parameters from nucleus to nucleus have been obtained by means of an unconventional absorption geometry, which has a dip in the radial distribution. The application of this geometry to other nuclei is being investigated, in particular to Mg, Al and Si.

Differential cross-sections and polarization measurements for 30 and 50 MeV protons scattered from $Cu^{63, 65}$ and of 50 MeV protons from Sm^{148} taken with the double focussing magnetic spectrometer on the PLA, have been analysed in terms of the standard and reformulated optical models. These data provide the first test of the latter at 50 MeV and typical fits to the Sm^{148} data are shown in figures 60 and 61.

Cross-section and asymmetry measurements have been made for the inelastic scattering of 30 MeV protons from the lowest 2^+ and 3^- states of $Zn^{64, 66, 68}$ and the first 2^+ states of $Mo^{92, 94, 96, 100}$. The analysis has been in terms of the Blair-Sherif model, in which the full grad term is used in the spin-orbit interaction (figure 62). The Mo elastic scattering data have been analysed with an optical model with a surface peaked real central term, and the results are being interpreted microscopically.

Angular distributions have been measured on the Variable Energy Cyclotron (VEC) for deuteron elastic scattering from $Sn^{112, 118, 124}$ at 20 MeV and $Sn^{112, 118, 119, 120}$ at 27 MeV, as little elastic scattering work has previously been done in this mass region with deuterons. More evidence has been found to favour a 100 MeV real well depth, mainly by comparing the resulting nuclear matter parameters with those obtained from proton scattering.

Fig. 59. The n-p elastic scattering cross-section for neutrons of 130 MeV measured in Experiment 34, compared with a previous measurement.

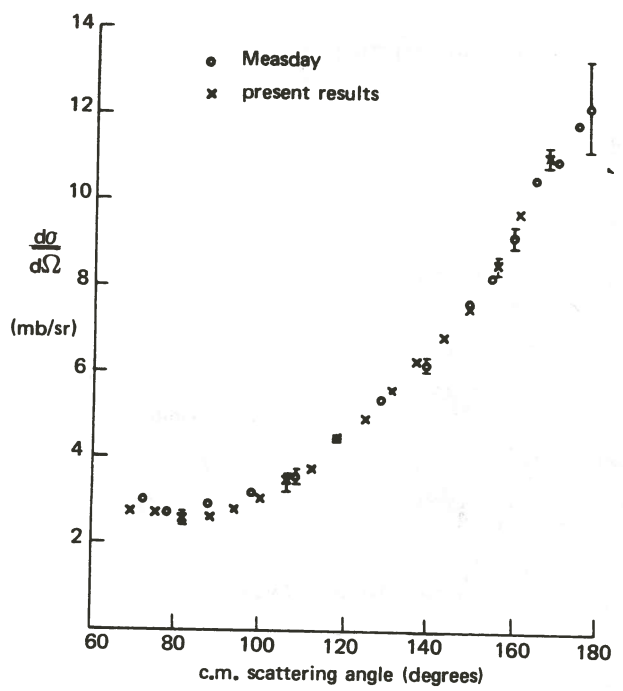

60. Fits to the differential cross-section data for the reaction Sm^{148}(p,p) Sm^{148} with standard and reformulated optical models. (Experiment 35).

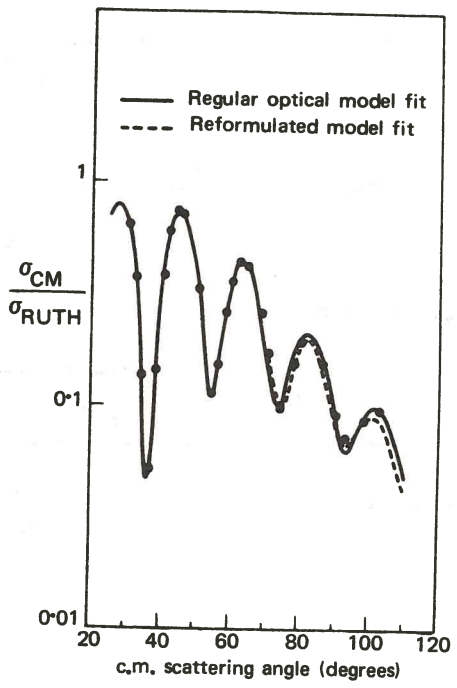

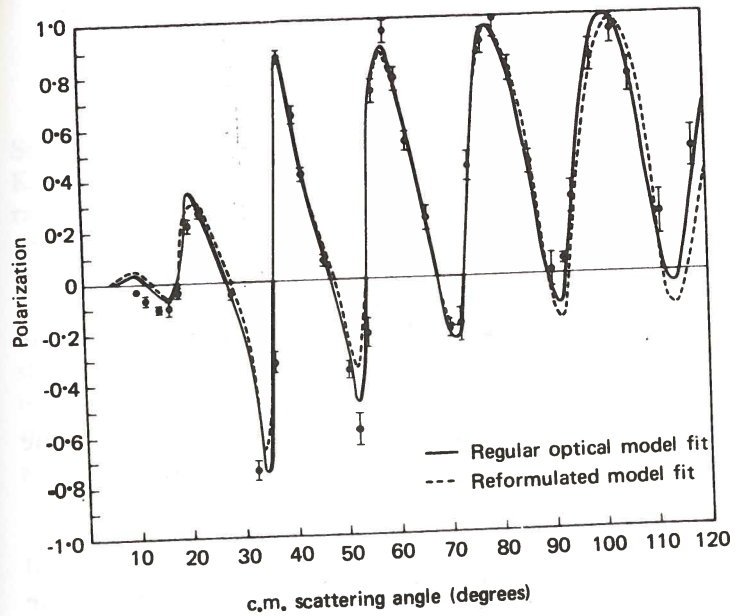

Figure 61. Fits to the polarization data for the reaction Sm^{148} (p,p) Sm^{148}. (Experiment 35).

Elastic and inelastic scattering of 53 MeV helions (He^3 ions) from Fe^{54} and Sm^{144} have been investigated on the VEC in order to provide more information on the interaction of complex particles with nuclei. This accurate data has helped to overcome some of the ambiguities usually present in complex particle scattering analysis.

The reaction Fe^{54} (h, d) Fe^{53} has been studied on the Harwell Tandem Generator using 18 MeV helions. The aim of this work is to investigate J dependence in these reactions and to obtain more information on the helion spin orbit interaction.

The group has participated in neutron scattering experiments on the 150 MeV Harwell Synchro-Cyclotron. These have consisted of p (n, pγ)n and n-d elastic scattering experiments. Preliminary information has been obtained on the d(n, 2n)p reaction and a feasibility study made for an n-d polarization experiment. (See Experiment 34).

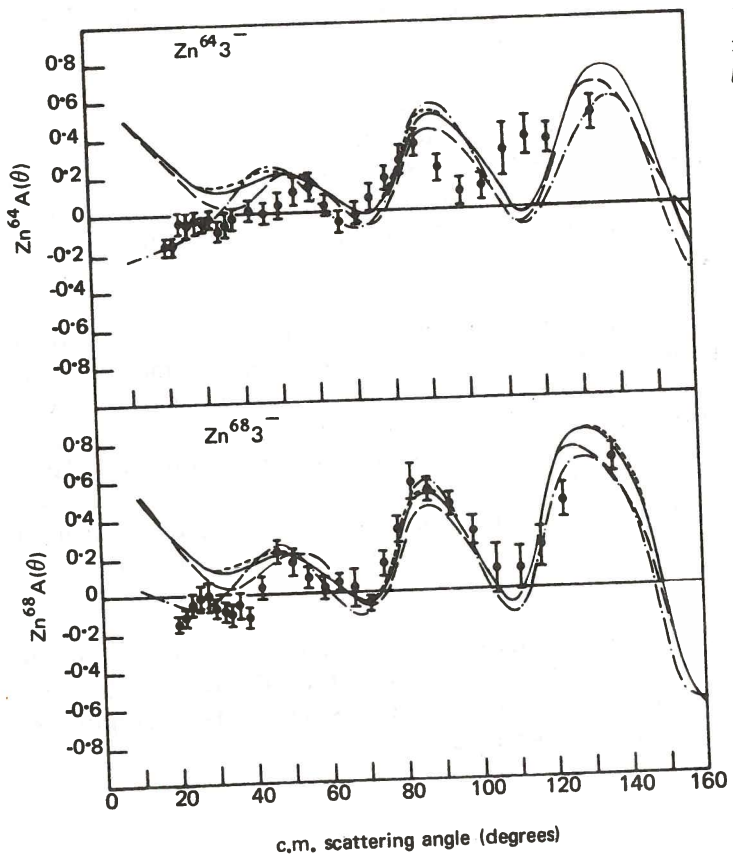

Fig. 62. Fits to $Zn^{64}3^-$ and $Zn^{68}3^-$ data. —.— Blair-Sherif model. ____ no spin orbit term. ____ simple radial term $\beta_{SO} = \beta_{real}$. ---- simple radial term $\beta_{SO} = 1{\cdot}25\beta_{real}$. (Experiment 35).

Theoretical High Energy Physics

The theory group works on a wide range of current problems, particularly in the realm of phenomenology – the confrontation of theory with experiment. This is thoroughly appropriate at the Rutherford Laboratory.

The interaction of theorists with experimenters was furthered by a series of informal two-day meetings at The Coseners House. The subjects were the Multi-particle Veneziano Model, Physics for the Omega Spectrometer, and Pion-Nucleon Resonances. About thirty participants from European centres were invited in each case. There was also the usual summer visitor programme.

The annual December conference this year was displaced into the first week of January, 1971. Over 200 physicists attended, mainly from British universities and laboratories.

The following brief accounts gives some idea of the interests of the group.

New Models for High-Energy Scattering. (ref. 6, 7.)

When the 70 GeV Serpukhov accelerator started working, more than doubling the highest available energy, surprising new results began to appear. The total cross-sections for $\pi^- p$ and $K^- p$ scattering, that had been steadily falling with increasing energy and were expected to go on falling, were found to level off at constant values above 30 GeV. This raised at least two questions:

(i) What new theoretical ingredient explains this levelling-off?

(ii) Since the $K^+ p$ cross-section is apparently constant up to the highest energies measured so far (20 GeV) and is considerably below the new constant $K^- p$ value, what has happened to the Pomeranchuk theorem that predicts asymptotic equality for these two cross-sections?

The Pomeranchuk theorem is not sacred. One of the assumptions on which it rests may be wrong, so failure of this theorem is an interesting possibility. But the Regge poles and Regge cuts that provide the usual language for discussing high energy scattering, happen to satisfy the Pomeranchuk theorem. So if the latter is to fail, some new ingredient must be added: Regge dipoles and singular cuts are among the suggestions made.

Alternatively, we may conjecture that whatever puts a kink in the $K^- p$ cross-section, changing its behaviour from a steady fall to a levelling-off, may also put a kink in the $K^+ p$ cross-section and cause it to start rising beyond 30 GeV, say – a region where it has not yet been measured. In this way the Pomeranchuk theorem could be preserved. We just have to find some ingredient to explain this kink. Here again there are many possibilities. Pole-cut cancellations, or an increasing component in the cross-section (behaving like ln E or ln $E)^2$ as energy $E \to \infty$) can all impart a kink. Complex Regge poles can give oscillations – repeated kinks, as it were.

Thus the Serpukhov data stimulate new thinking. The problem is to choose between the various new hypotheses. Fortunately, they lead to rather different predictions for other quantitites yet unmeasured, so that future experiments at Serpukhov and Batavia will help to distinguish between them.

$K_L \to K_S$ Regeneration Phase (ref. 5)

Simple Regge pole theory predicts that the phase of the amplitude for forward $K^0_L p \to K^0_S p$ regeneration should be near $-3\pi/4$, and experiments in the 2-8 GeV range confirm this value. However, preliminary results from Serpukhov suggest that the phase may change quite rapidly at higher energy, reaching perhaps $-\pi/4$ at 40 GeV. It is interesting to see if any of the new models being proposed to explain high energy cross-sections can also explain such a phase rotation. Several of them can. With violation of the Pomeranchuk theorem, the phase should go asymptotically to zero; whether it goes through $-\pi/4$ at 40 or 400 GeV is not determined – there is still a lot of freedom in such models. Models based on complex Regge poles also give a phase rotation, in the positive sense as observed.

The Line Reversal Puzzle

There are a set of line reversed reactions $ab \to cd$ and $\bar{c}b \to \bar{a}d$, of which the first is expected to have a real phase and the second a rotating phase, on the basis of dual Regge pole theory. Moreover, dual Regge poles predict the two cross-sections to be equal. Experimentally, however, the cross-section corresponding to the real phase seems always to be larger than the one corresponding to the rotating phase and this inequality is quantitatively significant for the hypercharge exchange processes. Modification of the Regge poles in terms of absorptive cuts generates an inequality, but in the wrong direction. If on the other hand the Regge poles are modified, in terms of colliding cuts, then the real amplitude gives the larger cross-section as observed. In fact a model based on pole-cut collision seems to fit the cross-section difference and polarization measurements quantiatively for hypercharge exchange processes.

Van Hove Plots (ref. 75)

The Van Hove Plot projects out the longitudinal components of phase-space which at high energy appear experimentally to contain most of the dynamical information while reducing the dimensionality of the problem. By this means several production processes were analysed in terms of a model which includes both Regge pole exchanges and their related phases at high subenergies and possible resonance formation at low energies. Besides Pomeron exchange, this analysis also stressed the importance of pion exchange in these reactions at the energies considered.

SU(3) Symmetry (ref. 85)

SU(3) has proved to be a very successful symmetry in classifying the observed particle spectrum and in relating three particle couplings. However the application of SU(3) predictions to scattering processes is difficult if the energies at which the comparisons are to be made are not specified. Prescriptions which involve superposing the thresholds in different reactions are only partially successful. For resonance decay, of course, the predictions are made at the resonance pole. Moreover the resonance masses can be prescribed by a simple formula, the Gell Mann-Okubo formula. It is natural therefore to try to extend this to a formula involving the energies at which comparison is to be made, this formula reducing to the Gell Mann-Okubo mass formula at the resonance poles. This prescription has been found to be successful in relating scattering processes.

Non-Linear SU(3) Symmetry

By treating SU(3) as a non-linear symmetry realised by the appearance of massless scalar mesons in the symmetry limit, and imposing Regge asymptotics on the scattering amplitudes of the theory, the usual algebraic consequences of SU(3) for vertices and masses are recovered. In addition there are new dynamical consequences for the couplings of a nonet of scalar mesons or perhaps instead for the tensor nonet of Regge trajectories at $\alpha = 0$.

Background to One-Pion Exchange, and Vector Dominance (ref. 58)

The notion of particle exchange goes back to the foundation of our subject; indeed, it is in this secondary role as 'virtual' quanta to mediate forces between other particles rather than in their primary role as free quanta, that a number of boson particles, notably pions, first impinged on our thinking (Yukawa, 1935). As is well known, the range of the force resulting from particle exchange is related to the exchanged mass by the 'Uncertainty Principle', i.e. Range = $\hbar$/(Mass x c), so that the lightest quanta correspond to the longest range. It is for this reason that the pion, the lightest strongly interacting particle, occupies a key place among exchanges. The 'Regge-picture' of high energy exchanges predicts a more sharply falling energy dependence for pion exchange than for rival mechanisms; none the less, pion exchange is conspicuous up to the highest observed energies.

Di-pion production and charged pion photo-production appear to be dominated by one pion exchange at small momentum transfer. In respect of di-pion production, this fact is exploited to infer $\pi\ \pi$ elastic scattering parameters upon which there exists very important and widely ramifying theoretical predictions from the notions of chirality and duality (di-pion production is essentially our only source of detailed $\pi\ \pi$ scattering information). In order for valid inferences to be made the background to one pion exchange has to be understood. As reported earlier, a simplified expression for the small t background has been developed involving rather few parameters. On fitting this parameterization to data at a number of beam momenta, a very simple behaviour for the transversely polarized rho background was noted. This was subsequently shown to conform to the predictions of the absorption model and the 'gauge invariant elastic Born' model and to be in agreement with 'Vector Dominance'.

Threshold Sum Rules from Unitarity (ref. 79)

The unitarity condition implies several constraints on the partial wave amplitudes, and these constraints may be converted into corresponding sum rules for the cross channel absorptive parts of scattering amplitudes. The super convergence and FESR relations (which are consequences of the absence of fixed poles in the angular momentum plane) and the unitary sum rules by Arbab and Slansky are typical examples. It has been shown that the unitarity condition may be explored further leading to sum rules for the crossed channel absorptive parts for fixed t at the respective two body threshold. It has been shown, using the t-channel unitarity condition, that the reduced partial wave $\pi\ \pi$ scattering amplitude evaluated at threshold for Re $\ell > -\frac{1}{2}$ vanishes and it has a known first derivative with respect to angular momentum ℓ at the point $\ell - \frac{1}{2}$. These properties imply sum rule constraints for the crossed channel absorptive part for t fixed at threshold. The sum rules have been analysed for $\pi\ \pi$ scattering. Their generalisation to other processes have also been investigated.

CP Non-Invariance in some Radiative K Decays

Work on possible CP-noninvariant effects in radiative $\tau^{\pm}$ decays has been extended to include effects of structure in the nonradiative amplitude and to consider also radiative $\tau'^{\pm}$ decays.

A systematic study of all possible tests for T- and CPT-invariances in the decays of individual neutral kaons in vacuum has been carried out. The importance of the various tests and their implications for the symmetry properties of interactions obeying different selection rules have been pointed out. These considerations, coupled with the known data on neutral kaon decays, lend support to the superweak theory of CP-nonconservation. Limits on possible CPT-(and T-) noninvariance of different interactions in neutral kaon decays are also being studied.

Sidewise Dispersion Relations (ref. 38)

Calculation of the anomalous magnetic moments of the nucleon from dispersion relations in the photon mass squared requires a knowledge of $\pi\ \pi \rightarrow N\bar{N}$ scattering below the physical threshold. On the other hand if we disperse in the nucleon mass squared, what is required is πN elastic scattering and πN photoproduction data in the physical region, so sidewise dispersion relations provide a better hope of calculating these quantities. Although the threshold region does not provide a satisfactory result, when the resonance region up to the limit of present scattering data is included, the experimental values of the magnetic moments are approximated.

Coulomb Corrections (ref. 52, 53)

Most scattering data refer to initial states of charged particles while in many cases the final states also involve charged particles. This means that a detailed study of these scattering processes entails treatment of both the strong and the electromagnetic interactions.

The inter-connection of the two interactions can be used to probe the electromagnetic structure of the scattered particles in simple cases such as $\pi^{\pm}N \rightarrow \pi^{\pm}N$. Alternatively, in the case of very accurate experiments this inter-connection must be taken into account when attempting to isolate information on the strong interaction.

The formulation for dealing with this situation has been developed for low energy πN scattering and it is being extended to cope with the low energy $K\bar{N}$ system.

Baryon Resonances (ref. 67)

Over the past few years the number of known particles and resonances has grown considerably, for example about ten years ago data compilations listed some seventeen states, now they list eighty with many more suspected to exist.

For the case of baryon resonances this increase has been largely due to the successful exploitation of the technique known as phase shift analysis. In this, one essentially analyses accurate two body scattering data in terms of amplitudes of known quantum numbers (spin, parity, isotopic spin etc.). By performing these anlyses at closely spaced mass intervals one is able to investigate structure which may be present and (hopefully!) isolate the resonant states. The major success to date with this technique has been in the field of pion-nucleon scattering below 2 GeV where the number of resonance states has grown from 4 in 1960 to 15 in 1970, with indications that there may still be more. The Rutherford Laboratory experimental teams have, since 1965, contributed of the order of half of the total world data used in these analyses, a very fine achievement. Currently Rutherford Laboratory teams (K13C, CERN SC23, K14A, π9, K15, K8) are engaged in measuring further pion nucleon two body scattering data to a far higher precision than obtained previously. Such data will go a long way to providing a complete picture of two body πN scattering below, say, 2 GeV, and when fully analysed should provide a wealth of new information.

At various times past members of the theory group have collaborated with experimental teams in phase shift analysing two body scattering data. In the last year these collaborators have been active in analysing both pion nucleon and kaon nucleon data.

'Exotic' Resonances (ref. 4, 80)

Currently much attention has been focused on K^+p scattering because here is a direct way of looking for strangeness + 1 resonances. A scheme which has been very successful in classifying known resonances is the quark model, where one invokes triplets of fractionally charged quarks to construct the baryon and their excited resonant states. The simplest of these models cannot easily accommodate low mass strangeness + 1 resonances, and so a strong test of such a model is whether such resonances exist. Recently, University College London have obtained

preliminary elastic K^+p scattering data between 1·4 and 2·3 GeV/c. Analysis of this data together with previous data has shown that a complete description of all currently available data can be obtained which does not require the existence of a strangeness + 1 resonance, at least with a mass less than 2·3 GeV.

A theoretical survey has also been made of the situation regarding the K^+p system and strangeness + 1 resonances, suggestions were made as to what might be the most valuable experiments to perform next. Further K^+p experimental work is being performed at the Rutherford Laboratory (K12, K15), the results of which are eagerly awaited.

Hyperon Resonances

Members of the theory group are also working on an analysis of strangeness - 1 kaon nucleon scattering. Systematic experimental data are now available over a wide range for the strangeness - 1 system for most two body final states. These various possible two body final states are related via unitarity (i.e. conservation of probability), but most analyses performed to date which take into account this relation have been restricted to the mass region below 1520 MeV. Work is now under way to extend such analyses into the mass range 1520 to 1720 MeV, where many resonant states are believed to exist. Values of the decay rates of the resonances into the various two body channels will be obtained the results being of relevance to the classification (e.g. in the quark models) of these states.

There is much work still to be done with the technique of phase shift analysis and, if the past progress is any guide, many exciting results should be forthcoming.

The A_2 Meson

One of the most exciting problems of the past year has been to understand the mass spectrum of the A_2 meson. Interest was aroused when the mass spectrum of the A_2^- meson, produced in the reaction $\pi^- p \rightarrow A_2^- p$, was found to have two closely spaced peaks with the separation between the peaks approximately equal to their width. The most widely accepted explanation of this phenomenon was that there exist two J = 2 mesons lying close in mass which interfere destructively to produce the dip. Of course the existence of a second spin two meson would pose many interesting questions as to its nature and the existence of its symmetry partners. In a subsequent experiment the A_2^+ was found to be unsplit, a fact that could be explained within the two meson hypothesis if the production of the A_2 meson included an isospin one component whose contribution would change sign between A_2^- and A_2^+ production. This would change the production phase to give no destructive interference for the A_2^+. This model would also explain the indications that A_2^o is split. However a recent experiment analysing the A_2^- at a much higher production energy has an unsplit mass plot and this is inconsistent with the simple picture presented above. It remains to be seen whether a plausible explanation of this new data is forthcoming or if indeed the two meson hypothesis is tenable at all.

The Y_0^* (1405)

The existing analyses of low energy $\bar{K}N$ scattering data parametrize the Y_0^* (1405), which lies between the $\Sigma\pi$ and $\bar{K}N$ thresholds, as a virtual bound state of these channels. However if the Y_0^* (1405) is interpretated as an isoscalar member of an SU(6) – L supermultiplet with orbital excitation $L = (1^-)$ it should be produced by the strong forces which give rise to the existence of the complete supermultiplet. Thus it should not be produced mainly by the $\bar{K}N$ and $\Sigma\pi$ channels. Re-analysis of the low energy $\bar{K}N$ data allowing different production mechanisms strongly suggest that the Y_0^* (1405) is indeed a virtual bound state of the $\bar{K}N$ and $\Sigma\pi$ channels and thus casts doubt on its supermultiplet interpretation.

Absorption from the Veneziano Model (ref. 31)

The infinite resonance spectrum given by the Veneziano model is perhaps suggestive that the model already includes the effect of numerous coupled channels. This hypothesis was used to determine the $\pi\pi$ and πK inelasticity parameters below 2 GeV from a partial wave dispersion relation. Approximating the integral over the left hand singularities by its Veneziano model equivalent, and assuming some plausible forms for the real parts of the phase-shifts, it was found there is considerable absorption above 1 GeV in the non-exotic channels.

Dual Model for πN Scattering (ref. 76)

Since the introduction of the Veneziano model for meson-meson scattering, several attempts have been made to construct a similar dual model for meson-baryon scattering. Among other difficulties, the apparent absence of parity doublets for leading baryon resonances is not easily reproduced. Recently, a prescription has been given for eliminating unwanted parity partners by introducing fixed J-plane cuts and constructing functions with poles in $S^{\frac{1}{2}}$ rather than in S. It is not clear, however that the resulting dual models can lead to a good description of πN scattering.

We have constructed explicitly a dual model which does not possess parity doublets along the leading trajectories. A feature of this model is that from one input trajectory it naturally produces two sets of degenerate baryon trajectories, half a unit apart. Mathematically it is simpler than previous models and we are able to analytically continue it to the physical region.

A Unitarised Veneziano Model (ref. 73)

An analysis has been carried out on a class of meson-baryon scattering processes using a form of unitarised Veneziano model. Unitarity is partly described by introducing all the coupled two-particle channels which are related to each other by the requirements of SU(3), duality, factorisation and absence of exotics. The Pomeron is interpreted as multi-particle absorptive corrections rather than as a t-channel exchange. The F/D ratio plays a particularly crucial role in understanding the behaviour of various reactions. To describe hypercharge exchange reactions, exchange-degeneracy breaking mechanisms are considered and evaluated.

Phenomenology based on the Veneziano Model (ref. 74)

Since its introduction two years ago much work has been done on the Veneziano model (this model was briefly discussed in the 1969 Annual Report). Despite its still rather serious drawbacks (e.g. it does not conserve probability, that is it does not obey unitarity) it is beginning to be used as a basis for phenomenological data fitting. One main area of application has been on 2 to 3 body reactions where early work showed (in one specific case) that a reasonable description of a lot of data could be obtained in a simple fashion (much to everyone's surprise!). A collaboration of theorists from CERN, Oxford and the Rutherford Laboratory have applied these ideas to all reactions involving the particles $K^+K^-\pi^-p\bar{n}$ and their charge conjugates. A qualitative description using a rather simple functional form has been obtained of a large body of data involving these particles. Also some interesting questions have been thrown up from this analysis concerning the dual nature of the pion Regge trajectory with low energy baryon resonances. By dual one means that in some sense a description of scattering data can either be in terms of the pion Regge trajectory or in terms of a sum of baryon resonances. It has been shown by the analysis that possibly the pion trajectory is not dual to known baryon resonances.

Antiproton Annihilation

The annihilation of antiprotons on nucleons are being investigated. A description of the 3-meson final state in terms of invariant amplitudes has been found, and is being used to inter-relate the various $\bar{p}p$ and $\bar{p}n$ final states.